Electronic Supplementary Material (ESI) for ChemComm.

Controlling Photocatalytic Reduction of CO_2 in Ru(II)/Re(I) Dyads via Linker Oxidation State

Christopher M. Brown,[1] Thomas Auvray,[2] Emile E. Deluca,[1] Maria B. Ezhova,[1] Garry S. Hanan[2] and Michael O. Wolf[1]

1. *Department of Chemistry, 2036 Main Mall, University of British Columbia, Vancouver, BC, V6T 1Z1, Canada*
2. *Département de Chimie, Université de Montréal, Montréal, QC, H3T 1J4, Canada*

Experimental Details

General

All experiments were conducted under air unless otherwise stated. Solvents used for synthesis were of reagent grade and were used without any further purification. HPLC grade solvents were used for spectroscopic studies. Microwave reactions were performed in a Biotage Initiator 2.5 microwave synthesizer. 5,6-epoxy-5,6-dihydro-[1,10]-phenanthroline, ruthenium(III) chloride and 30% H_2O_2 solutions were purchased from Sigma-Aldrich. Niobium carbide was purchased from Alfa Aesar. All reagents were used as received, and *cis*-$Ru(phen)_2Cl_2$ was prepared as per the literature.[1] Sacrificial reductant 1,3-Dimethyl-2-phenyl-2,3-dihydro-1H-benzo[d]imidazole (BIH),[2] and catalyst $Re(phen)(CO)_3Br$[3] were synthesized according to the literature.

Spectroscopy

^1H, $^{13}C\{^1H\}$, COSY, ROESY, HSQC and HMBC NMR spectra were collected using Bruker NMR spectrometers and referenced first to TMS and then to the residual protonated solvent peak. Pro-ligand spectra were collected on a Bruker AV-400 spectrometer, spectra of the monometallic species on a Bruker AV-600 spectrometer, and spectra of the mixed-metal systems on a Bruker AV-850 spectrometer. NMR solvents (from Aldrich) were used as received. Electrospray ionization mass spectrometry data was obtained using a Bruker Esquire LC ion trap mass spectrometer. Infrared spectroscopy was performed on an attenuated total reflection (ATR) crystal using a Perkin-Elmer Frontier FT-IR spectrometer. UV-vis absorption spectra were recorded on a Varian-Cary 5000 UV-Vis-near-IR spectrophotometer. Fluorescence data were collected on a Photon Technology International (PTI) QuantaMaster 50 fluorimeter fitted with an integrating sphere, double excitation monochrometer and utilizing a 75 W Xe arc lamp as the source. Emission lifetime data were collected using a Horiba Yvon Fluorocube TCSPC apparatus. A 453 nm NanoLED was used as the excitation source, pulsing at a repetition rate of 100 kHz. Broadband emission was monitored by a CCD detector at wavelengths >550 nm using a low-pass filter. Data were fitted using the DAS6 Data Analysis software package. Sample solutions were first sparged with Ar for 30 min and then maintained under a blanket of Ar for the duration of the measurements in 1 cm^2 quartz cells (Starna Cells) fitted with a rubber septum.

Electrochemistry

All electrochemical measurements were performed using a Metrohm Autolab PGSTAT12 potentiostat in an air-tight single compartment cell with an $Ag/AgNO_3$ pseudo reference electrode. A 7 mm^2 glassy carbon disc was used as the working electrode and a platinum mesh was used as the counter electrode. Each experiment was carried out in a N_2 sparged CH_3CN solution with 0.1 M *n*-Bu_4NPF_6 (recrystallized 4× from EtOH) as the supporting

electrolyte. Potentials were referenced to an internal Fc/Fc^+ standard that was added to the analyte solution subsequent analytical measurements. The working electrode was regenerated and cleaned between measurements by polishing with alumina paste, followed by successive sonication treatments in H_2O and acetone. All measurements were performed at a 1 mM concentration of analyte, with the exception of the Re monometallic species, which were analyzed at lower concentrations (~0.5 mM) due to the limited solubility of these complexes in CH_3CN.

All cyclic voltammetry measurements were performed with a scan rate of 100 mVs^{-1} and square wave voltammetry measurements were performed with a 25 Hz wave form. The effect of uncompensated resistance on voltametric measurements was minimized with a positive feedback circuit in the potentiostat.

Computational Details

Calculations were made with Gaussian16 rev.B.01,[4] using the PBE0 hybrid functional[5] with LanL2DZ as the basis set.[6–9] The optimizations were conducted without symmetry constraints, followed by frequency calculations to confirm that energy minima had been reached in all cases. The energy, oscillator strength, and related MO contributions for singlet–singlet and singlet–triplet excitations were obtained from the TD-DFT/singlets and the TD-DFT/triplets output files, respectively, for the S_0-optimized geometry. GaussView6 and Chemissian4.53[10] were used for data analysis, visualization and surface plots. All calculations were conducted for CH_3CN-solvated complexes using a conductor-like polarized continuum (CPCM) solvation model.[11]

Photocatalytic Studies

Gas evolution was followed in real-time using a PerkinElmer Clarus-580 gas chromatograph (GC) equipped with a 7' HayeSep N60/80 pre-column, a 9' molecular sieve 13 V45/60 column and both a thermal conductivity detector (for H_2 detection) and a flame ionization detector (for CO and CH_4 detection). Argon was used as the carrier and eluent gas. Amounts of H_2, CO and CH_4 were quantified using a calibration curve established using standardized a gas mixes (500 ppm H_2, 50 ppm CO, 50 ppm CH_4 in N_2, and 250 ppm H_2, 50 ppm CO, 50 ppm CH_4 in N_2). The error associated with the detected values were estimated to be 10%. In a typical experiment, a vial was placed on top of a green LED (530 nm centered) set to an approximate 30 mW output, in an aluminum cast connected to a thermostatic bath set at 20 °C. It was sealed with a rubber septum pierced with two stainless steel tubes. The first tube carried a CO_2 flow pre-bubbled in DMF. The flow was set at 10 ml/min (adjusted with calibrated mass flow MCseries from Alicat) and referenced with a digital flowmeter (Perkin Elmer FlowMark). The second tube led the flow to the GC sample loop through a 2 ml overflow protection vial, then through an 8-port stream select valve (VICCI) and finally to GC sample loop. A microprocessor (Arduino Uno) coupled with a custom PC interface allowed for timed injections.

Synthetic Methods

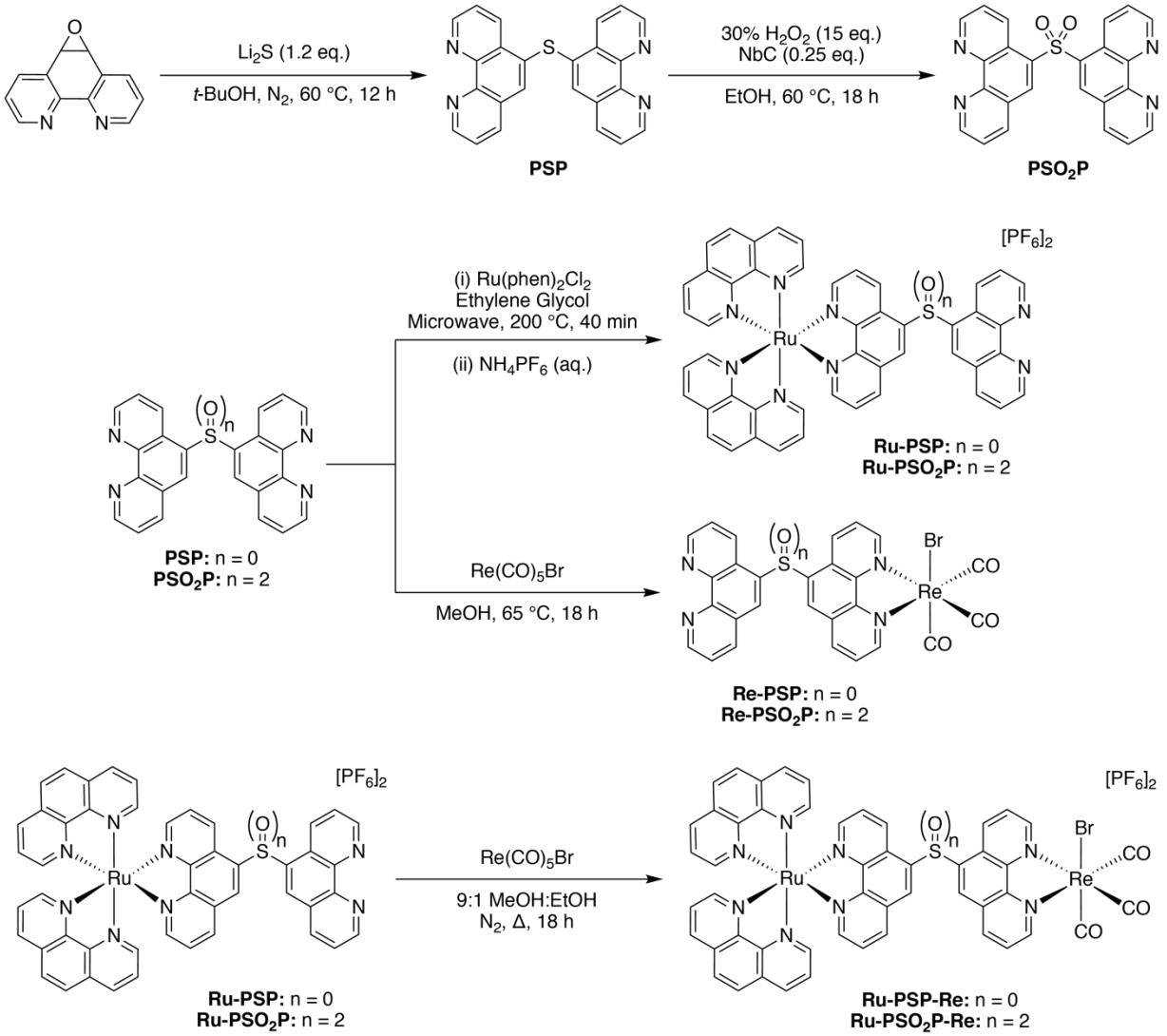

Scheme S1 Synthetic methods to the pro-ligands, monometallic, and bimetallic species discussed in this work.

Synthesis and Characterization of Pro-Ligands

The series of ligands described in this work was prepared using modifications of previously reported procedures (Scheme S1). Ligand **PSP** was prepared in a one-pot synthesis through reaction of Li_2S with commercially available 5,6-epoxy-5,6-dihydro-1,10-phenanthroline in refluxing *tert*-butanol.[12] This pro-ligand was then oxidized to the sulfone (**PSO_2P**) analogue with 30% H_2O_2 in the presence of a NbC catalyst.[13] Both bridging pro-ligands were isolated in moderate to high yields and structural characterization performed using ^1H, $^{13}C\{^1H\}$, COSY, HSQC and HMBC NMR experiments, in addition to mass spectrometry and infrared spectroscopy.

Synthesis and Characterization of Mono- and Bi-Metallic Species

cis-$Ru(phen)_2Cl_2$ was synthesized as per the literature.[1] Monometallic Ru(II) complexes **Ru-PSP** and **Ru-PSO_2P** were prepared using an adapted procedure from Johansson *et al*. utilizing a microwave synthesizer.[14] *cis*-$Ru(phen)_2Cl_2$ was reacted with an excess of the desired pro-ligand (Scheme S1) and the crude products purified *via* column chromatography over silica gel (F60) using CH_3CN:H_2O:KNO_3 (aq.) as the eluting solvent. The pure products were isolated as hexafluorophosphate salts through the addition of a saturated aqueous NH_4PF_6 solution that resulted in the formation of precipitates that were orange in color in all cases. Monometallic rhenium complexes **Re-PSP** and **Re-PSO_2P** were synthesized by reaction of the desired pro-ligand with $Re(CO)_5Br$ in MeOH heated to reflux in the dark. Purification occurred *via* column chromatography using silica gel (F60) using first CH_3CN then 98:2 CH_2Cl_2:MeOH as the eluting solvents. Bridged Ru(II)-Re(I) species were prepared through reaction of **Ru-PSP** or **Ru-PSO_2P** with $Re(CO)_5Br$ under a nitrogen atmosphere in the dark followed by purification over silica gel in a similar manner to the monometallic Ru(II) species. ^1H and ^{13}C NMR spectra were assigned using ^1H, $^{13}C\{^1H\}$, COSY, ROESY, HSQC and HMBC experiments. The HR-MS spectra show product peaks corresponding to $[M-PF_6]^+$ exhibiting characteristic ruthenium and rhenium isotope patterns.

Experimental Details

di(1,10-phenanthrolin-5-yl)sulfane (PSP)

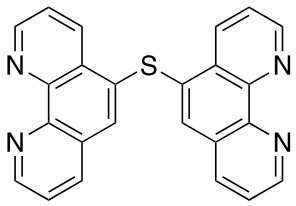

While under an N_2 atmosphere, a solution of Li_2S (0.591 g, 12.8 mmol, 1.2 equiv.) in *tert*-butanol (250 mL) was added dropwise to a suspension of 5,6-epoxy-5,6-dihydro-[1,10]-phenanthroline (2.10 g, 10.7 mmol, 1.0 equiv.) in *tert*-butanol (60 mL) at 60 ºC over a 40 minute period. The reaction was monitored by TLC (silica gel; EtOAc:MeOH:NH_4OH 10:1:0.5) and subsequently stirred for 18 h at 60 ºC, following which the solvent was removed under reduced pressure and the crude product dissolved in $CHCl_3$ (300 mL) and washed with sat. NH_4Cl (40 mL). The aqueous layer was then further extracted with $CHCl_3$ (3 × 100 mL) and the combined organics washed with brine (2 × 100 mL). The organic layer was dried with $MgSO_4$, filtered and the solvent removed *in vacuo*. The resulting crude solid was recrystallized from MeOH:H_2O (2:1) giving off-white needles (2.72 g, 6.95 mmol, 65%). The spectroscopic and spectrometric data matches that of the literature.[12] ^1H NMR (400 MHz, $CDCl_3$) δ 9.30 (dd, *J* = 4.4, 1.6 Hz, 2H), 9.23 (dd, *J* = 4.4, 1.7 Hz, 2H), 8.79 (dd, *J* = 8.4, 1.6 Hz, 2H), 8.05 (dd, *J* = 8.2, 1.7 Hz, 2H), 7.74 – 7.68 (m, 4H), 7.64 (dd, *J* = 8.1, 4.4 Hz, 2H). HR-ESI MS: *m/z* calcd. for $C_{24}H_{15}N_4S$: 391.1017; Found: 391.1015 $[M+H]^+$.

5,5´-sulfonylbis(1,10-pheananthroline) (PSO_2P)

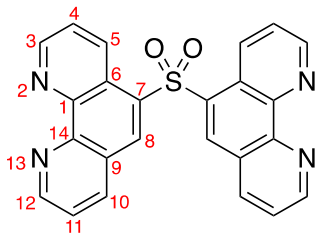

To EtOH (50 mL) was added **PSP** (0.496 g, 1.27 mmol, 1.0 equiv.), NbC (0.033 g, 0.320 mmol, 0.25 equiv.) and 30% H_2O_2 solution (1.90 mL, 19.1 mmol, 15.0 equiv.). The reaction mixture was then heated to 60 ºC for 18 h. After cooling to room temperature, sat. $Na_2S_2O_3$ solution (25 mL) was added, followed by H_2O (75 mL), forming a white precipitate which was extracted with EtOAc (3 × 30 mL). The combined organics were washed with H_2O (30 mL) and brine (30 mL), dried over $MgSO_4$, filtered and the solvent removed under reduced pressure to give a white solid that required no further purification (0.510 g, 1.21 mmol, 95%). ^{1}H NMR (400 MHz, $CDCl_3$*d*) δ 9.37 (dd, *J* = 4.4, 1.7 Hz, 2H, H_3), 9.21 (dd, *J* = 4.3, 1.6 Hz, 2H, H_{12}), 9.05 (dd, *J* = 8.6, 1.6 Hz, 2H, H_{10}), 8.90 (s, 2H, H_8), 8.46 (dd, *J* = 8.1, 1.7 Hz, 2H, H_5), 7.81 (dd, *J* = 8.1, 4.4 Hz, 2H, H_4), 7.63 (dd, *J* = 8.6, 4.3 Hz, 2H, H_{11}). ^{13}C{^{1}H} NMR (101 MHz, $CDCl_3$) δ 153.86 (C_3), 151.37 (C_{12}), 148.14 (C_1), 146.58 (C_{14}), 138.00 (C_5), 134.83 (C_8), 133.06 (C_{10}), 131.98 (C_7), 125.94 (C_6), 124.41 (C_4), 123.80 (C_{11}), 123.59 (C_9). IR (neat): $\tilde{\nu}$ (σ SO_2) 1288 and 1126 cm^{-1}. HR-EI MS: *m/z* calcd. for $C_{24}H_{14}N_4O_2S$: 422.0837; Found: 422.0834 $[M]^+$.

$[Ru(phen)_2(PSP)][PF_6]_2$ (Ru-PSP)

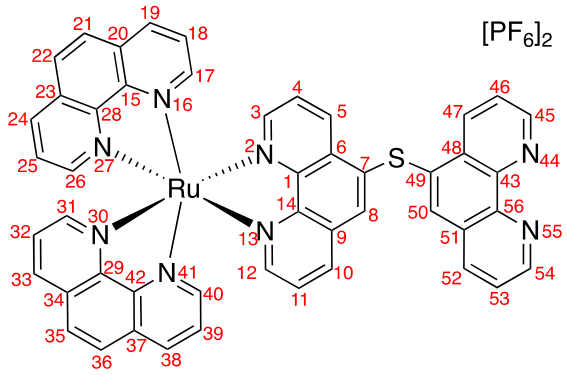

To a microwave vial was added $Ru(phen)_2Cl_2$ (0.470 g, 0.883 mmol, 1.0 equiv.), and **PSP** (0.383 g, 0.981 mmol, 1.11 equiv.) and ethylene glycol (11 mL). The suspension was reacted in a microwave for 40 min at 200 ºC and cooled to room temperature, following which the solvent was diluted with H_2O (80 mL) and NH_4PF_6 added to precipitate the crude compound. The resulting orange precipitate was filtered and washed with H_2O and Et_2O and then purified using column chromatography (silica gel, F60) using CH_3CN:H_2O:KNO_3 (aq.) (88:8:10) as the eluting solvent. The first major orange band was collected. After an ion exchange with NH_4PF_6 the pure product was isolated as an orange solid (0.439 g, 0.385 mmol, 44%). ^{1}H NMR (600 MHz, CD_3CN) δ 9.20 (dd, *J* = 4.3, 1.7 Hz, 1H, H_{12}), 9.18 (dd, *J* = 4.4, 1.6 Hz, 1H, H_3), 8.97 (dd, *J* = 8.5, 1.2 Hz, 1H, H_{47}), 8.74 (dd, *J* = 8.2, 1.7 Hz, 1H, H_5), 8.59 (tdd, *J* = 15.9, 8.3, 1.3 Hz, 4H, $H_{19,24,33,38}$), 8.37 (dd, *J* = 8.0, 1.7 Hz, 1H, H_{10}), 8.35 (s, 1H, H_8), 8.26 (d, *J* = 0.7 Hz, 2H, $H_{35,36}$), 8.23 (d, *J* = 2.1 Hz, 2H, $H_{21,22}$), 8.12 (dd, *J* = 8.4, 1.2 Hz, 1H, H_{52}), 8.09 (dd, *J* = 5.3, 1.2 Hz, 1H, H_{45}), 8.07 (dd, *J* = 5.2, 1.3 Hz, 1H, H_{17}), 8.04 (dd, *J* = 5.2, 1.2 Hz, 1H, H_{40}), 8.01 (dd, *J* = 5.2, 1.3 Hz, 1H, H_{31}), 7.98 (dd, *J* = 5.4, 1.3 Hz, 1H, H_{26}), 7.90 (dd, *J* = 5.3, 1.3 Hz, 1H, H_{54}), 7.78 (dd, *J* = 8.1, 4.3 Hz, 1H, H_{11}), 7.72 – 7.64 (m, 5H, $H_{4,18,39,46,50}$), 7.62 (dd, *J* = 8.2, 5.2 Hz, 1H, H_{32}), 7.59 (dd, *J* = 8.2, 5.3 Hz, 1H, H_{25}), 7.42 (dd, *J* = 8.4, 5.2 Hz, 1H, H_{53}). ^{13}C{^{1}H} NMR (151 MHz, CD_3CN) δ 154.47 (C_{45}), 154.10 (C_{40}), 154.04 (C_{17}), 153.92 (C_{31}), 153.86 (C_{26}), 153.45 (C_{54}), 152.41 (C_{12}), 151.61 (C_3), 149.38 (C_{43}), 148.81 ($C_{15,28,29,42}$), 148.11 ($C_{1,56}$), 147.79 (C_{14}), 137.78 ($C_{19,24,33,38}$), 137.22 (C_{10}), 136.56 (C_8), 136.41 (C_{52}), 134.82 (C_5), 134.40 (C_{47}), 131.95 ($C_{20,23,34,37}$), 131.58 (C_{51}), 130.48 (C_{49}), 129.60 (C_9), 129.18 ($C_{6,48}$), 129.01 ($C_{35,36}$), 128.98

($C_{21,22}$), 127.55 (C_{50}), 127.43 (C_{7}), 127.13 (C_{53}), 126.95 (C_{46}), 126.83 ($C_{18,39}$), 126.80 ($C_{25,32}$), 124.90 (C_{11}), 124.76 (C_{4}). MALDI-TOF MS: *m/z* calcd. for $C_{48}H_{30}F_6N_8PRuS$: 991.1028; Found: 991.1032 $[M–PF_6]^+$.

[Ru(phen)$_2$(PSO$_2$P)][PF$_6$]$_2$ (Ru-PSO$_2$P)

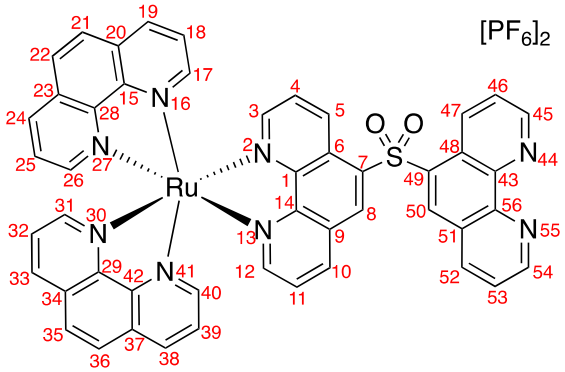

Ru(phen)$_2$Cl$_2$ (0.284 g, 0.533 mmol, 1.0 equiv.) and **PSO$_2$P** (0.250 g, 0.591 mmol, 1.1 equiv.) and ethylene glycol (15 mL) were heated in a microwave at 200 ºC for 40 min. The reaction was cooled to room temperature and the ethylene glycol diluted with H_2O (80 mL). NH_4PF_6 was added to a stirred solution of the reaction mixture, following which the precipitate was filtered and washed with H_2O and Et_2O. The crude product was purified using column chromatography (silica gel, F60) using CH_3CN:H_2O:KNO_3 (aq.) (88:8:10) as the eluting solvent where the first major orange band was collected, which after anion exchange with NH_4PF_6 yielded the pure complex as an orange powder (0.130 g, 0.111 mmol, 21%). ^{1}H NMR (600 MHz, CD_3CN) δ 9.39 (s, 1H, H_8), 9.25 (d, *J* = 4.4 Hz, 2H, $H_{50,54}$), 9.19 (dd, *J* = 8.8, 1.2 Hz, 1H, H_{47}), 9.14 – 9.11 (m, 2H, $H_{3,5}$), 8.81 (dd, *J* = 8.3, 1.3 Hz, 1H, H_{10}), 8.72 (dd, *J* = 8.2, 1.8 Hz, 1H, H_{52}), 8.60 – 8.52 (m, 4H, $H_{19,24,32,38}$), 8.22 (s, 2H, $H_{21,36}$), 8.20 (s, 2H, $H_{22,35}$), 8.14 (dd, *J* = 5.4, 1.3 Hz, 1H, H_{12}), 7.99 (dd, *J* = 5.4, 1.2 Hz, 1H, H_{45}), 7.93 (ddd, *J* = 6.9, 5.2, 1.3 Hz, 3H, $H_{17,31,40}$), 7.91 (dd, *J* = 5.3, 1.3 Hz, 1H, H_{26}), 7.87 (dd, *J* = 8.1, 4.3 Hz, 1H), H_{53}, 7.71 (m, 2H, $H_{4,11}$), 7.59 (dd, *J* = 8.4, 5.4 Hz, 1H, H_{39}), 7.57 – 7.53 (m, 3H, $H_{25,32,46}$), 7.51 (dd, *J* = 8.3, 5.2 Hz, 1H, H_{18}). ^{13}C{^{1}H} NMR (151 MHz, CD_3CN) δ 156.95 (C_{12}), 154.90 (C_{45}), 154.70 (C_{54}), 154.21 (C_{17}), 154.19 (C_{40}), 153.86 (C_{31}), 153.77 (C_{26}), 151.85 (C_3), 151.14 (C_{14}), 149.87 (C_{43}), 148.92 (C_{56}), 148.70 ($C_{15,42}$), 148.64 ($C_{28,29}$), 147.33 (C_1), 139.70 (C_{52}), 139.31 (C_{10}), 137.91 ($C_{19,38}$), 137.88 (C_{24}), 137.85 (C_{33}), 137.73 (C_{49}), 135.00 (C_{50}), 134.56 (C_{47}), 134.40 (C_8), 134.05 (C_5), 131.96 ($C_{30,37}$), 131.90 ($C_{23,34}$), 129.61 (C_9), 128.99 ($C_{21,36}$), 128.97 ($C_{22,35}$), 127.84 (C_{11}), 127.39 (C_{46}), 127.25 (C_{48}), 127.19 (C_{51}), 126.82 (C_{32}), 126.80 (C_{25}), 126.69 (C_{34}), 126.66 (C_{18}), 125.46 (C_{53}), 124.83 (C_4), 124.41 (C_7). IR (neat): $\tilde{\nu}$ (σ SO_2) 1312 and 1136 cm^{-1}. MALDI-TOF MS: *m/z* calcd. for $C_{48}H_{30}F_6N_8O_2PRuS$: 1023.0930; Found: 1023.0928 $[M–PF_6]^+$.

Re(PSP)(CO)$_3$Br (Re-PSP)

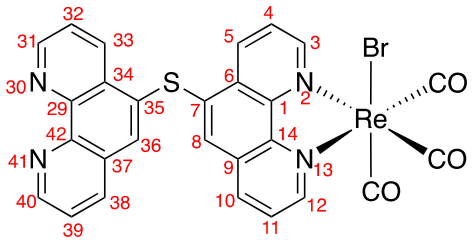

PSP (0.231 g, 0.599 mmol, 1.32 equiv.) was dissolved in refluxing MeOH (250 mL), to which $Re(CO)_5Br$ (0.185 g, 0.455 mmol, 1.0 equiv.) in 90 mL MeOH was added dropwise. The solution left to reflux for 18 h in the dark, following which the reaction mixture was cooled to room temperature and the solvent removed *via* rotary evaporation. The crude powder was purified using column chromatography (silica gel, F60) first using CH_3CN, followed by 98:2 CH_2Cl_2:MeOH, giving a yellow solid. (0.149 g, 0.201 mmol, 44%). ^{1}H NMR (600 MHz, $CDCl_3$) δ 9.50 (ddd, *J* = 8.3, 5.1, 1.3 Hz, 1H, H_3), 9.33 (dd, *J* = 4.4, 1.7 Hz, 1H, H_{12}), 9.30 (dd, *J* = 4.3, 1.6 Hz, 1H, H_{31}), 9.27 (ddd, *J* = 7.1,

5.0, 1.4 Hz, 1H, H_{40}), 9.07 (ddd, *J* = 8.5, 5.6, 1.4 Hz, 1H, H_5), 8.69 (ddd, *J* = 8.4, 6.7, 1.7 Hz, 1H, H_{33}), 8.29 (dd, *J* = 8.1, 1.7 Hz, 1H, H_{10}), 8.25 (s, 1H, H_8), 8.05 (td, *J* = 8.4, 1.4 Hz, 1H, H_{38}), 7.98 (ddd, *J* = 8.4, 5.1, 3.2 Hz, 1H, H_4), 7.75 (dd, *J* = 8.0, 4.4 Hz, 1H, H_{11}), 7.70 (ddd, *J* = 8.4, 6.0, 4.5 Hz, 2H, $H_{32,39}$), 7.24 (s, 1H, H_{36}). $^{13}C\{^1H\}$ NMR (151 MHz, $CDCl_3$) δ 153.86 (C_3), 152.83 (C_{40}), 152.08 (C_{12}), 151.54 (C_{31}), 147.44 (C_1), 146.82 (C_{14}), 146.70 (C_{29}), 146.06 (C_{38}), 136.83 (C_{42}), 136.66 (C_{10}), 136.11 (C_8), 134.90 (C_3), 134.24 (C_{33}), 130.42 (C_{37}), 129.49 (C_7), 128.44 (C_{35}), 128.41 (C_9), 126.36 (C_{39}), 126.10 (C_4), 125.28 (C_{36}), 124.44 (C_{31}), 124.20 (C_{11}). IR (neat): $\tilde{\nu}$ (σ CO) 2019, 1884 and 1866 cm^{-1}. HR-EI MS: *m/z* calcd. for $C_{27}H_{15}BrN_4O_3ReS$: 738.9578; Found: 738.9575 $[M]^+$.

Re(PSO$_2$P)(CO)$_3$Br (Re-PSO$_2$P)

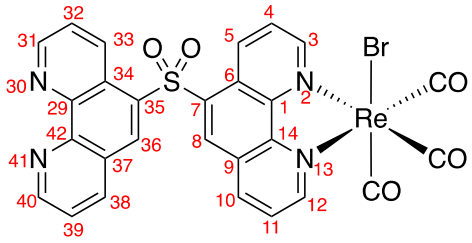

To a MeOH (250 mL) solution heated to reflux of **PSO$_2$P** (0.239 g, 0.566 mmol, 1.48 equiv.) was added dropwise a MeOH (90 mL) solution of $Re(CO)_5Br$ (0.155 g, 0.382 mmol, 1.0 equiv.). The reaction was heated at reflux for 18 h in the absence of light, following which the solution was cooled to room temperature and the solvent removed *in vacuo*. The crude solid was then using column chromatography (silica gel, F60) using first CH_3CN followed by 98:2 CH_2Cl_2:MeOH as the eluting solvents, yielding an orange powder. (0.145 g, 0.188 mmol, 49%). ^1H NMR (600 MHz, $CDCl_3$) δ 9.53 (ddd, *J* = 8.6, 5.2, 1.4 Hz, 1H, H_{12}), 9.48 – 9.44 (m, 1H, H_3), 9.43 – 9.39 (m, 2H, $H_{5,40}$), 9.28 (dd, *J* = 4.3, 1.6 Hz, 1H, H_{31}), 9.04 (ddd, *J* = 8.6, 3.4, 1.6 Hz, 1H, H_{33}), 8.97 (d, *J* = 2.3 Hz, 1H, H_{36}), 8.81 (d, *J* = 1.3 Hz, 1H, H_8), 8.65 (ddd, *J* = 8.2, 6.3, 1.4 Hz, 1H, H_{10}), 8.53 (dt, *J* = 8.2, 1.8 Hz, 1H, H_{38}), 7.98 (ddd, *J* = 8.4, 5.1, 3.7 Hz, 1H, H_{11}), 7.92 (ddd, *J* = 8.7, 5.1, 4.0 Hz, 1H, H_4), 7.85 (dd, *J* = 8.1, 4.4 Hz, 1H, H_{39}), 7.72 (ddd, *J* = 8.6, 4.3, 1.5 Hz, 1H, H_{32}). $^{13}C\{^1H\}$ NMR (151 MHz, $CDCl_3$) δ 156.07 (C_{12}), 154.47 (C_{40}), 154.43 (C_3), 151.82 (C_{31}), 148.83 (C_{14}), 148.26 (C_{42}), 147.73 (C_1), 139.59 (C_{10}), 138.43 (C_{38}), 137.68 (C_7), 135.71 (C_5), 133.36 (C_{36}), 133.29 (C_{33}), 133.16 (C_{35}), 131.22 (C_8), 128.24 (C_9), 127.11 (C_{11}), 126.80 (C_4), 126.37 (C_6), 125.97 (C_{37}), 124.81 (C_{39}), 124.38 (C_{32}), 123.64 (C_{34}). IR (neat): $\tilde{\nu}$ (σ SO_2) 1304 and 1126 cm^{-1}; $\tilde{\nu}$ (σ CO) 2016, 1884 and 1865 cm^{-1}. HR-EI MS: *m/z* calcd. for $C_{27}H_{15}BrN_4O_5ReS$: 770.9476; Found: 770.9484 $[M]^+$.

[Ru(phen)$_2$(PSP)Re(CO)$_3$Br][PF$_6$]$_2$ (Ru-PSP-Re)

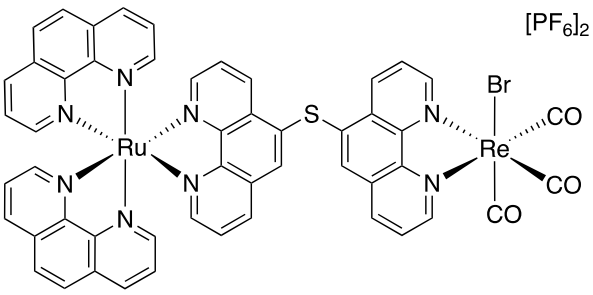

A round-bottomed flask was charged with **Ru-PSP** (0.426 g, 0.373 mmol, 1.0 equiv.) and $Re(CO)_5Br$ (0.181 g, 0.448 mmol, 1.2 equiv.) and placed under an N_2 atmosphere. A 9:1 MeOH:EtOH (500 mL) solution was added and the reaction mixture refluxed for 18 h in the dark then cooled to room temperature, following which the solvent was removed *in vacuo*. The crude product was purified over silica gel (F60) with a CH_3CN:H_2O:KNO_3 (aq.) (95:5:5) solvent system. The nitrate salt of the complex underwent a salt metathesis with NH_4PF_6 and was filtered, yielding an orange powder. (0.466 g, 0.299 mmol, 80%). ^1H NMR (850 MHz, CD_3CN) δ 9.49 (dddd, *J* = 16.1, 10.8, 5.0, 1.3 Hz, 2H),

9.43 (dddd, *J* = 11.6, 8.0, 5.0, 1.4 Hz, 2H), 9.19 – 9.06 (m, 2H), 8.96 – 8.89 (m, 2H), 8.70 – 8.52 (m, 11H), 8.37 – 8.25 (m, 10H), 8.21 (s, 1H), 8.19 (s, 1H), 8.14 – 8.07 (m, 7H), 8.05 – 7.96 (m, 10H), 7.72 – 7.68 (m, 4H), 7.68 – 7.62 (m, 6H), 7.57 (dddd, *J* = 14.2, 9.3, 5.6, 1.2 Hz, 2H). $^{13}C\{^{1}H\}$ NMR (214 MHz, CD_3CN) δ 156.28, 156.27, 155.11, 155.10, 155.02, 154.95, 154.93, 154.87, 154.73, 154.68, 154.66, 149.81, 149.75, 149.08, 148.88, 148.87, 148.86, 148.85, 148.66, 148.63, 148.62, 148.27, 148.25, 147.91, 147.85, 147.83, 140.56, 140.53, 139.60, 139.57, 139.52, 139.47, 138.50, 138.48, 137.89, 137.88, 137.86, 137.85, 137.84, 137.52, 137.47, 137.44, 137.38, 136.98, 136.90, 136.88, 135.05, 134.96, 134.87, 133.83, 133.77, 133.75, 133.69, 133.64, 133.61, 133.36, 133.29, 133.28, 133.22, 133.16, 132.68, 132.59, 132.53, 132.45, 132.42, 132.38, 132.19, 132.16, 132.07, 132.06, 132.04, 132.02, 132.01, 131.69, 131.59, 131.56, 131.51, 131.49, 131.45, 131.43, 131.29, 131.21, 131.16, 131.08, 130.92, 129.10, 129.08, 129.05, 128.20, 128.20, 128.10, 128.09, 127.78, 127.75, 127.72, 127.66, 127.64, 127.63, 127.60, 127.41, 127.39, 127.37, 127.28, 127.26, 127.24, 126.91, 126.90, 126.88, 126.85. IR (neat): $\tilde{\nu}$ (σ CO) 2022, 1913 and 1894 cm^{-1}. MALDI-TOF MS: *m/z* calcd. for $C_{51}H_{30}BrF_6N_8O_3PRuReS$: 1346.9588; Found: 1346.9583 $[M–PF_6]^+$.

$[Ru(phen)_2(PSO_2P)Re(CO)_3Br][PF_6]_2$ (Ru-PSO_2P-Re)

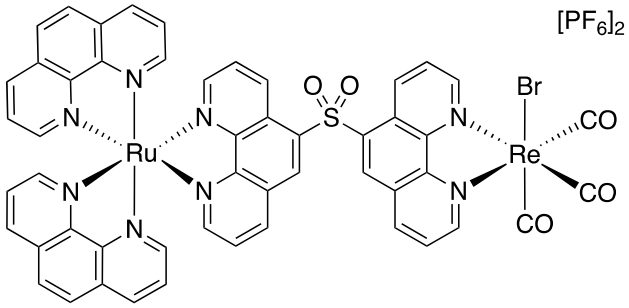

Under an N_2 atmosphere, and in the absence of light, **Ru-PSO_2P** (0.127 g, 0.108 mmol, 1.0 equiv.) and $Re(CO)_5Br$ (0.053 g, 0.130 mmol, 1.2 equiv.) were heated to reflux for 18 h in a 9:1 MeOH:EtOH (500 mL) solution. Following cooling, the solvents were removed under reduced pressure and the crude residue purified using column chromatography over silica gel (F60) with CH_3CN:H_2O:KNO_3 (aq.) (95:5:5) as the eluting solvent. The product was converted to the hexafluorophosphate salt through addition of NH_4PF_6 (aq.) and then filtered, yielding an orange solid. (0.129 g, 0.105 mmol, 97%). ^{1}H NMR (850 MHz, CD_3CN) δ 9.56 (dt, *J* = 5.2, 0.9 Hz, 1H), 9.56 – 9.54 (m, 2H), 9.53 (s, 1H), 9.50 (s, 2H), 9.46 (dt, *J* = 5.1, 1.0 Hz, 2H), 9.40 (tt, *J* = 7.7, 1.1 Hz, 2H), 9.17 (dt, *J* = 8.9, 0.9 Hz, 2H), 9.06 (td, *J* = 8.7, 1.4 Hz, 2H), 8.88 (dt, *J* = 8.4, 1.6 Hz, 2H), 8.62 – 8.60 (m, 3H), 8.58 (dddd, *J* = 6.6, 4.7, 3.3, 1.1 Hz, 4H), 8.57 – 8.55 (m, 1H), 8.26 (d, *J* = 0.6 Hz, 2H), 8.25 (s, 2H), 8.23 (d, *J* = 0.8 Hz, 2H), 8.22 – 8.18 (m, 4H), 8.14 – 8.13 (m, 1H), 8.13 – 8.11 (m, 1H), 8.03 (ddd, *J* = 7.0, 5.2, 1.1 Hz, 2H), 8.01 – 7.98 (m, 3H), 7.97 (td, *J* = 5.3, 1.5 Hz, 3H), 7.95 – 7.93 (m, 4H), 7.77 (d, *J* = 5.5 Hz, 1H), 7.76 (d, *J* = 5.4 Hz, 1H), 7.64 – 7.59 (m, 7H), 7.59 – 7.57 (m, 1H), 7.57 – 7.55 (m, 1H), 7.55 – 7.53 (m, 1H). $^{13}C\{^{1}H\}$ NMR (214 MHz, CD_3CN) δ 159.32, 158.88, 157.06, 157.05, 156.70, 156.68, 155.88, 155.85, 155.81, 155.77, 155.53, 155.49, 155.46, 155.45, 153.10, 153.07, 151.62, 151.43, 150.37, 150.35, 150.34, 150.32, 150.31, 150.29, 150.15, 143.84, 143.80, 141.15, 139.65, 139.62, 139.59, 139.58, 139.55, 139.54, 138.57, 138.55, 138.51, 138.50, 138.44, 138.06, 138.05, 137.21, 137.10, 137.04, 137.02, 136.12, 136.04, 135.99, 133.65, 133.63, 133.62, 133.58, 131.31, 131.29, 131.06, 131.04, 130.67, 130.66, 130.63, 130.57, 129.98, 129.95, 129.61, 129.59, 129.56, 129.54, 129.26, 129.20, 128.85, 128.84, 128.71, 128.67, 128.50, 128.48, 128.47, 128.38, 128.37,

128.32, 128.28. IR (neat): $\tilde{\nu}$ (σ SO_2) 1322 and 1140 cm^{-1}; $\tilde{\nu}$ (σ CO) 2022, 1914 and 1889 cm^{-1}. MALDI-TOF MS: *m/z* calcd. for $C_{51}H_{30}BrF_6N_8O_5PRuReS$: 1373.9474; Found: 1373.9476 $[M–PF_6]^+$.

Structural Characterization of Ru(II)–Re(I) Dyads

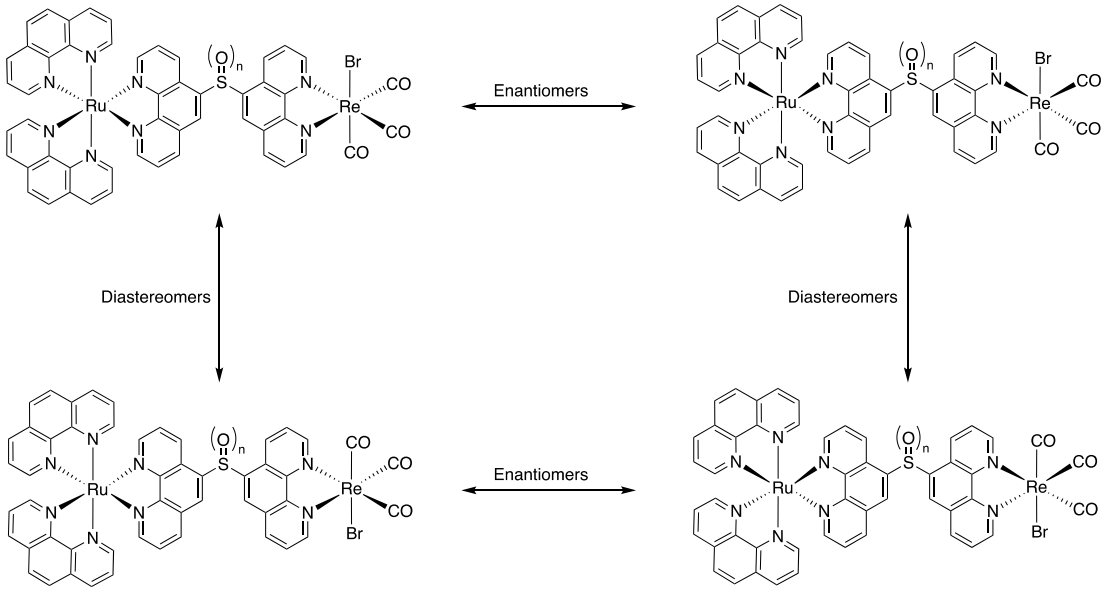

Scheme. S2 Stereoisomers of Ru(II)-Re(I) dyads. n = 0 or 2.

The protons in the 6- and 6´-positions on the **PSO_2P** bridge are singlets in ^1H NMR with signals at δ = 9.50 and δ = 8.23 for the phenanthroline moieties bound at Ru and Re, respectively. ROESY experiments observing through-space correlations between the bridge and the phen ligands bound to the Ru center were used to determine the binding of **PSO_2P**. The singlet seen at each position is in fact two overlapping signals (for the two diastereomers) as determined from HSQC experiments (Fig. S1b) indicating that the proton signal corresponds to two separate carbon environments. From COSY, ROESY, HSQC, HMBC and $^{13}C\{^1H\}$ experiments it was possible to distinguish the bridging ligands of the two distinct isomers.

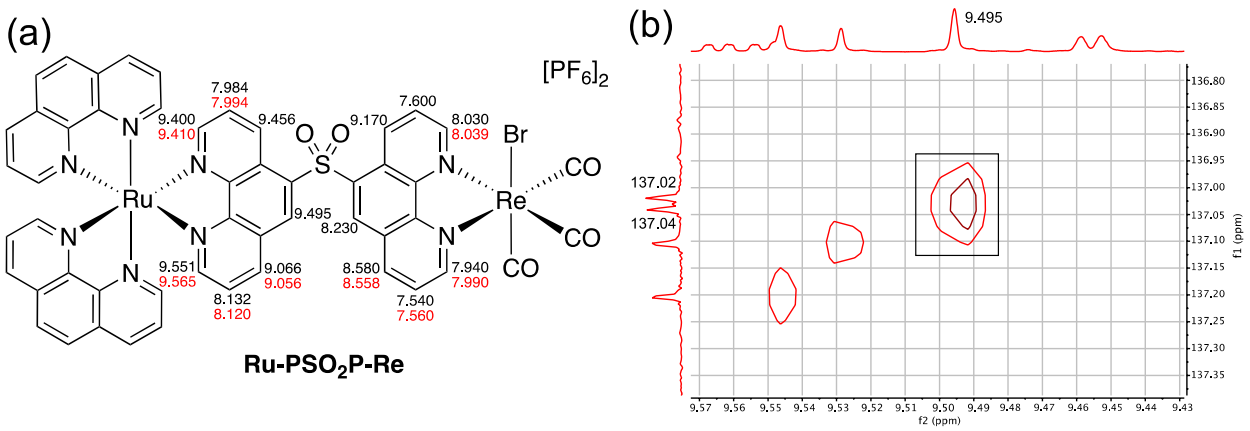

Fig. S1 (a) ^{1}H NMR shifts for the bridging ligand in **Ru-PSO$_2$P-Re**. Black text designates signals from one diastereotopic species, red text for the other. Chemical shifts with only one number indicates overlapping, indistinguishable species. (b) ^{1}H–^{13}C HSQC NMR spectrum (CD_3CN, 850 MHz, 25 °C) showing two diastereotopic carbon signals correlating to one broad singlet in the 6-position of the sulfur-bridged phenanthroline ligand bound at the Ru center.

Electrochemical Data

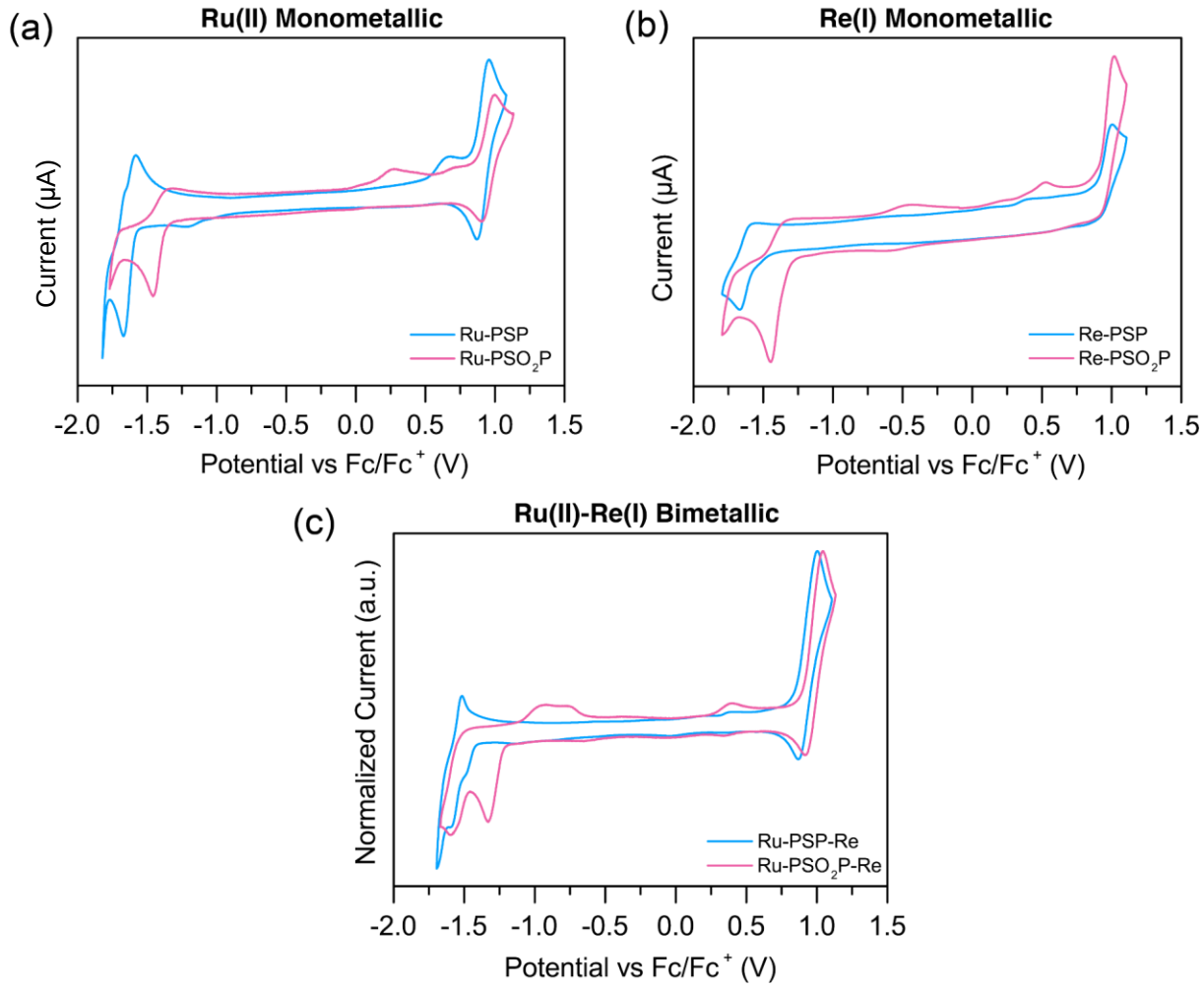

Fig. S2 Cyclic voltammograms of (a) Ru(II) monometallic complexes; (b) Re(I) monometallic complexes; (c) Ru(II)–Re(I) bimetallic species. All spectra taken in dry, N_2-sparged CH_3CN solutions at room temperature.

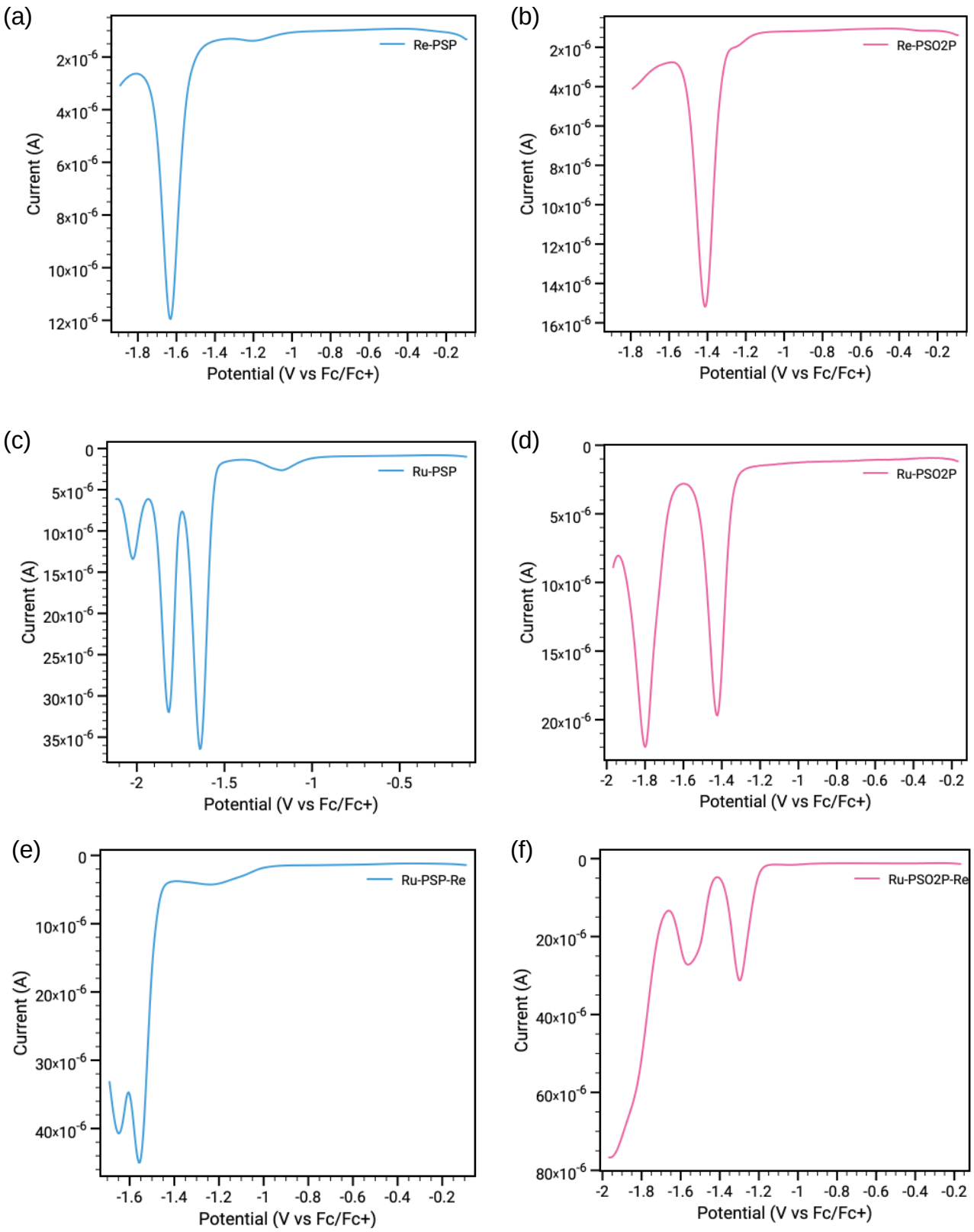

Fig. S3 Square wave voltammograms of Re(I) and Ru(II) monometallic complexes, and Ru(II)-Re(I) dyads. All spectra taken in dry, N_2-sparged CH_3CN solutions at room temperature.

Photophysical Data

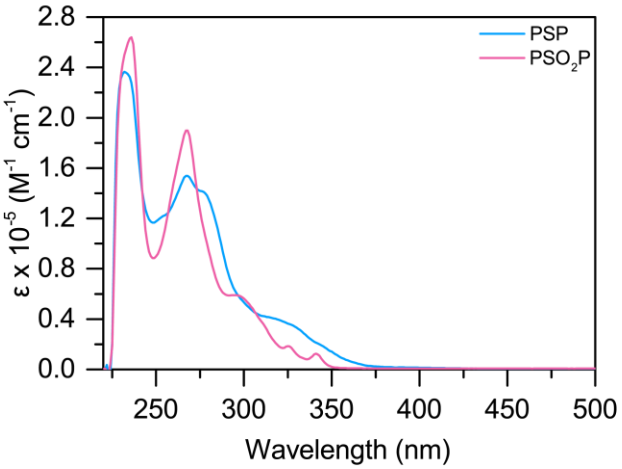

Fig. S4 Absorption spectra of **PSP** and **PSO_2P** in CH_2Cl_2 solutions at room temperature.

Table S1 Absorption values of **PSP** and **PSO_2P**.

	λ_{abs} (nm)
PSP	233, 267, 283sh, 319, 350sh [a]
PSO_2P	237, 267, 200, 326, 341 [a]

[a] Measured in $CHCl_3$ at 25 °C.

Table S2 Radiative (k_r) and non-radiative (k_{nr}) rate constants of Ru-containing complexes.[a]

	k_r	**knr**
Ru-PSP	1.04 x 10^5	9.71 x 10^5
Ru-PSO_2P	7.00 x 10^4	3.85 x 10^5
Ru-PSP-Re	8.35 x 10^4	7.04 x 10^5
Ru-PSO_2P-Re	5.75 x 10^4	6.27 x 10^5

[a] Measured in CH_3CN at 25 ºC.

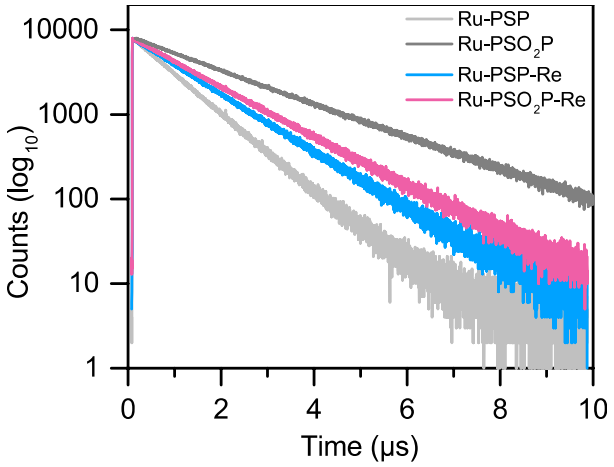

Fig S5. Photoluminescence lifetime data for Ru-containing monometallic and bimetallic species (λ_{ex} = 453 nm). CH_3CN solutions of concentration ~3×10^{-6} M sparged with Ar at 25 °C.

Computational Calculations

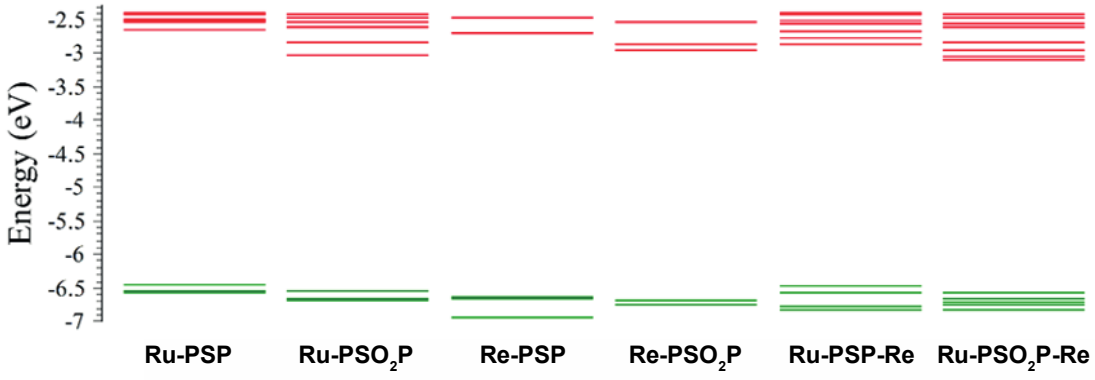

Fig. S6 Energy level diagram for the different Ru(II) and Re(I) monometallic complexes, and Ru(II)-Re(I) dyads.

Table S3 Frontier orbitals of the different complexes

	HOMO	**LUMO**
Ru-PSP	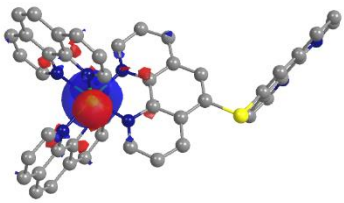 –6.469 eV	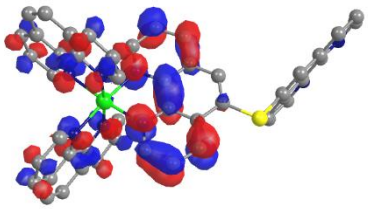 –2.680 eV

Ru-PSO$_2$P	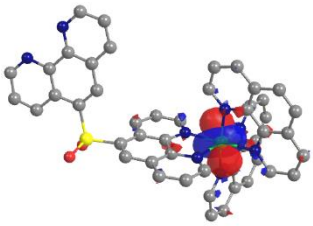 –6.569 eV	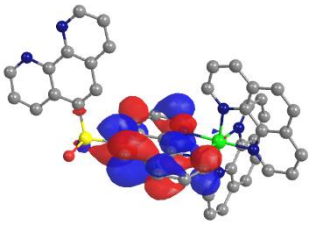 –3.047 eV
Re-PSP	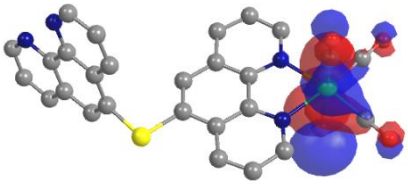 –6.654 eV	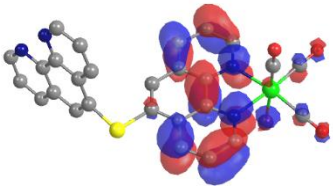 –2.716 eV
Re-PSO$_2$P	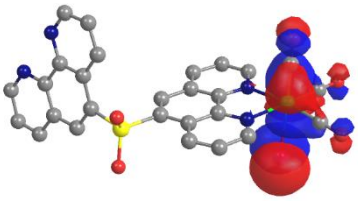 –6.702 eV	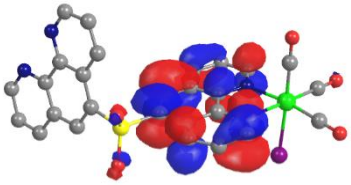 –2.965 eV
Ru-PSP-Re	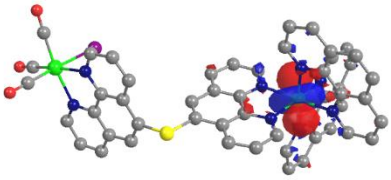 –6.480 eV	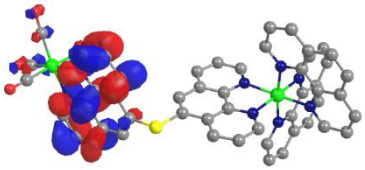 –2.882 eV
Ru-PSO$_2$P-Re	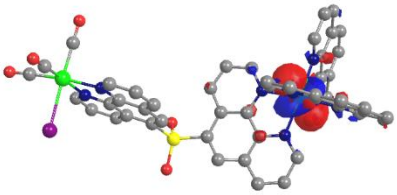 –6.581 eV	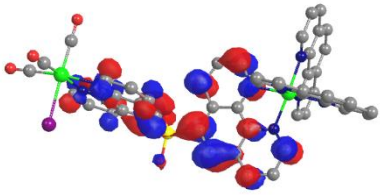 –3.107 eV

Table S4 Natural transition orbitals for the lowest singlet–singlet transition of each complex.

	Hole	Particle
Ru-PSP (460 nm) ^{1}MLCT Ru→ PSP	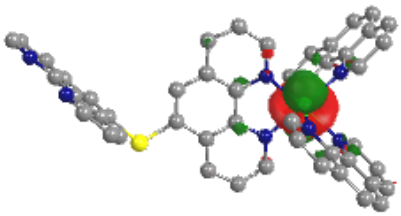	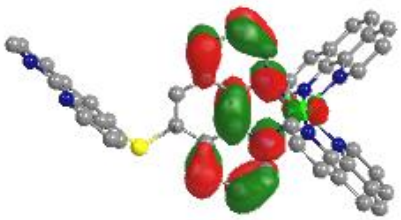
Ru-PSO$_2$P (484 nm) ^{1}MLCT Ru→ PSOP	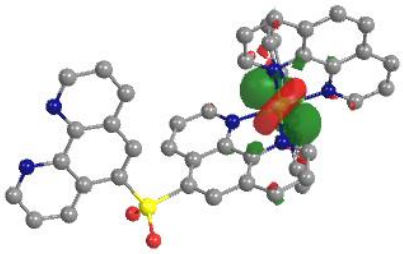	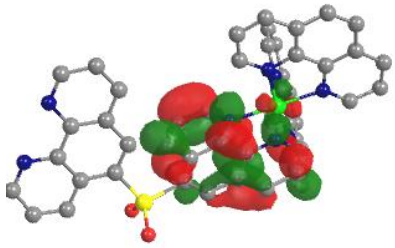
Re-PSP (415 nm) ^{1}MLLCT {ReCO$_3$Br}→ PSP	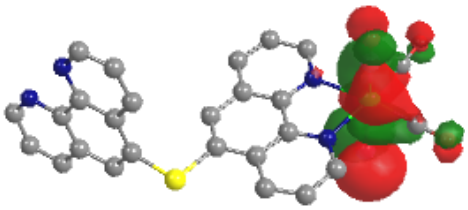	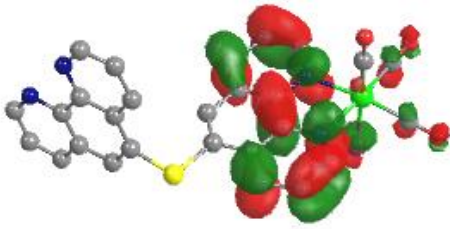
Re-PSO$_2$P (434 nm) ^{1}MCLT {ReCO$_3$Br}→ PSOP	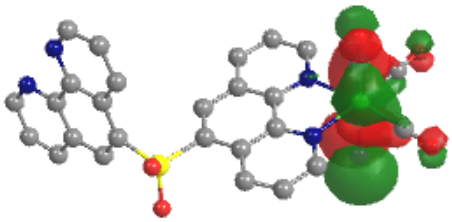	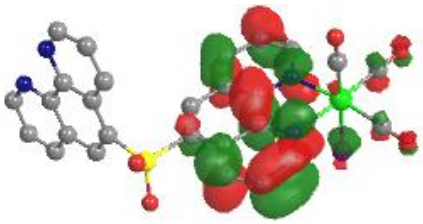
Ru-PSP-Re (462 nm) ^{1}MCLT Ru→ PSP	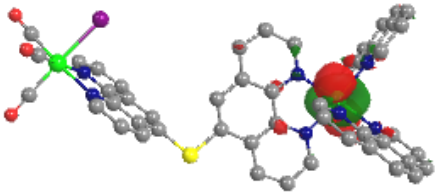	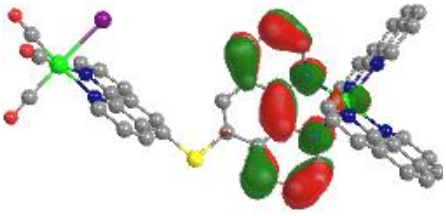
Ru-PSO$_2$P-Re (488 nm) ^{1}MCLT Ru→ PSOP	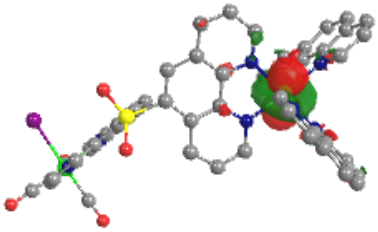	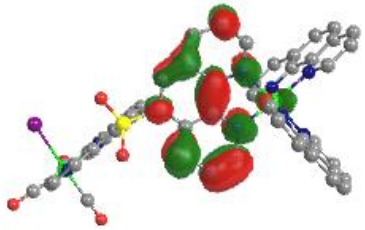

Table S5 Natural transition orbitals for the lowest singlet–triplet transition of each complex.

	Hole	**Particle**
Ru-PSP (537 nm) 52/41 ^{3}MLCT Ru (d) → PSP (π*) ^{3}ILCT {S} → PSP ^{3}LC PSP (π) → PSP (π*)	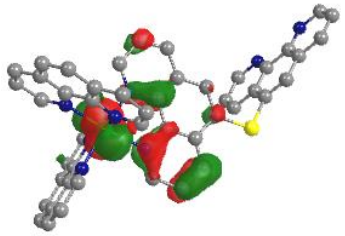 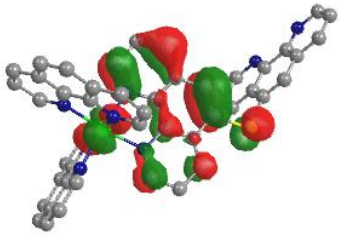	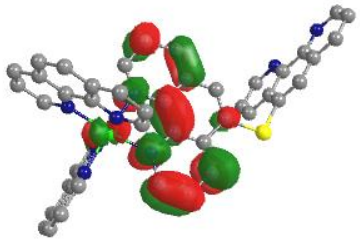 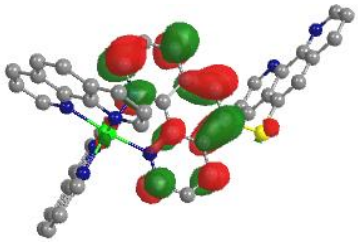
Ru-PSO$_2$P (552 nm) 68/29 ^{3}MLCT Ru (d) → PSP (π*) ^{3}LC PSOP (π) → PSO$_2$P (π*)	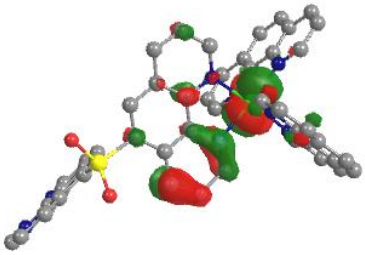 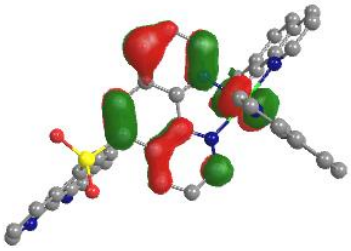	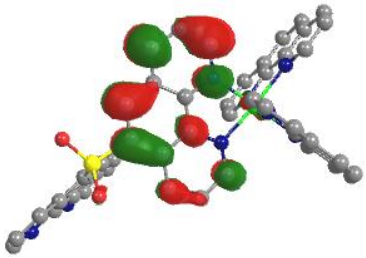 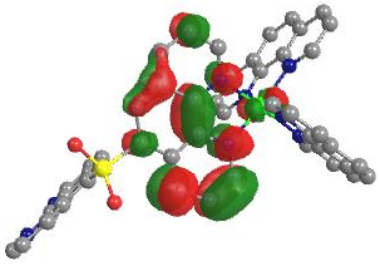

Re-PSP (498 nm) 74/21 ^{3}MCLT {$ReCO_3Br$}→ PSP ^{3}ILCT {S} → PSP ^{3}LC PSP (π) → PSP (π*)	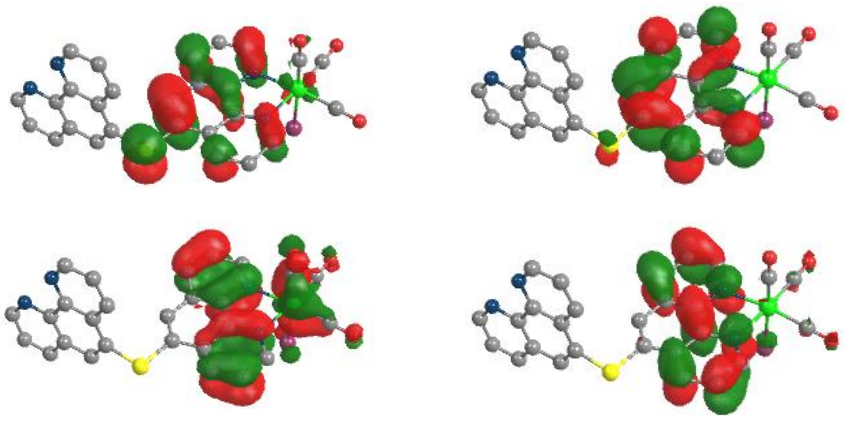
Re-PSO_2P (484 nm) 55/39 ^{3}MCLT {$ReCO_3Br$}→ PSO_2P ^{3}LC PSP (π) → PSO_2P (π*)	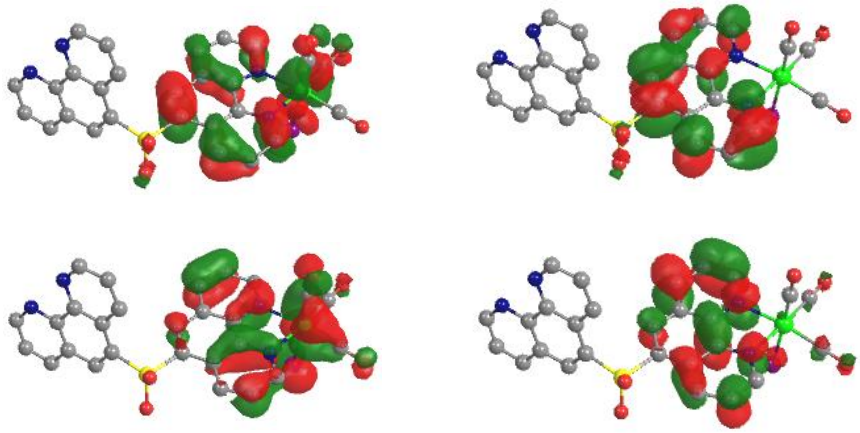
Ru-PSP-Re (537 nm) 54/40 ^{3}MLCT Ru (d) → PSP (π*) ^{3}ILCT {S} → PSP ^{3}LC PSP (π) → PSP (π*)	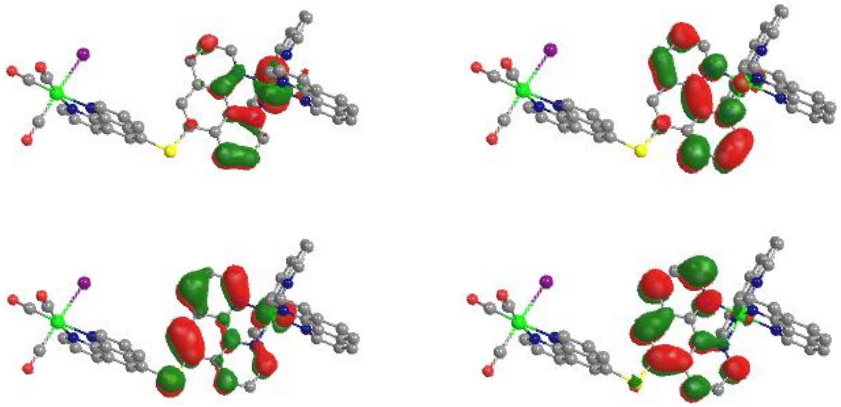

Ru-PSO$_2$P-Re (555 nm) 69/28 ^{3}MLCT Ru (d) → PSO$_2$P (π*) ^{3}LC PSOP (π) → PSO$_2$P (π*)	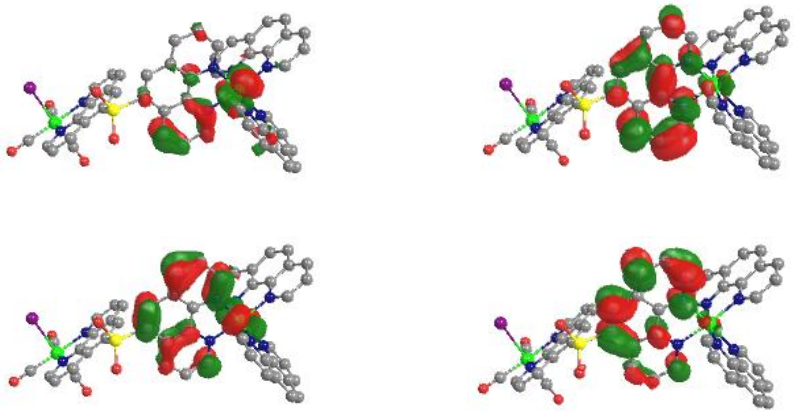

Table S6 Optimized geometry coordinates of Ru-PSP.

Center	Atomic	Coordinates (Å)			Center	Atomic	Coordinates (Å)		
Number	Number	X	Y	Z	Number	Number	X	Y	Z
1	1	0.724966	2.494185	-3.522391	45	1	-2.612508	-5.428828	-2.290196
2	6	0.714362	1.930490	-2.597347	46	6	-2.523396	-4.420584	-1.899029
3	1	2.851476	1.968154	-2.306372	47	7	-2.281900	-1.796208	-0.901419
4	6	1.892408	1.637987	-1.921148	48	6	-3.429479	-3.961234	-0.910426
5	7	-0.607299	0.784808	-0.940197	49	6	-1.433297	-2.256281	-1.837341
6	6	1.827632	0.896685	-0.714100	50	6	-3.265760	-2.638541	-0.437937
7	6	-0.522468	1.490189	-2.081871	51	6	-4.498204	-4.760078	-0.369980
8	6	0.552094	0.495438	-0.262198	52	1	-0.668691	-1.575104	-2.187774
9	6	2.982035	0.545328	0.061975	53	6	-5.345635	-4.255317	0.583818
10	1	-1.448557	1.704771	-2.598921	54	1	-4.621991	-5.774974	-0.734780
11	6	2.868467	-0.184829	1.218587	55	1	-6.149874	-4.865171	0.983551
12	1	3.953311	0.877217	-0.290790	56	6	-5.189767	-2.912414	1.078675
13	6	1.569311	-0.608573	1.703155	57	6	-6.026511	-2.332872	2.065342
14	6	1.355832	-1.358404	2.886865	58	6	-4.142166	-2.116192	0.560641
15	6	0.425988	-0.248093	0.949739	59	6	-5.784384	-1.027596	2.476894
16	6	0.059511	-1.693397	3.258442	60	1	-6.842869	-2.907729	2.490292
17	1	2.192546	-1.673737	3.500826	61	1	-6.403064	-0.552570	3.228678
18	1	-0.132929	-2.265036	4.158129	62	6	-4.715716	-0.299358	1.914073
19	6	-1.027173	-1.289530	2.459783	63	1	-4.509811	0.715693	2.228165
20	1	-2.043782	-1.535391	2.737070	64	7	-3.907072	-0.826883	0.978397
21	7	-0.853048	-0.582769	1.329629	65	1	-1.732028	4.068475	3.356266
22	44	-2.309336	0.072332	0.003159	66	1	-0.818673	-3.881511	-3.110453
23	6	-2.228289	3.730472	2.454583	67	16	4.316807	-0.642585	2.244671
24	1	-3.308718	5.565738	2.108189	68	1	5.182002	-4.014812	-1.589556
25	6	-3.102465	4.558705	1.760625	69	6	5.722583	-3.111099	-1.333128
26	7	-2.558997	1.939017	0.876336	70	1	4.475317	-2.586549	0.340600
27	6	-3.728402	4.072558	0.585362	71	6	5.331995	-2.314786	-0.267025
28	6	-1.976586	2.423980	1.986778	72	7	7.571813	-1.627925	-1.823040
29	6	-3.421232	2.753263	0.179581	73	6	6.065425	-1.140118	0.039271
30	6	-4.652697	4.841023	-0.206974	74	6	6.852946	-2.724298	-2.089071
31	1	-1.303511	1.764035	2.518500	75	6	7.200998	-0.832816	-0.775331
32	6	-5.229018	4.310529	-1.333532	76	6	5.713757	-0.253311	1.125051
33	1	-4.887492	5.853422	0.106878	77	1	7.181088	-3.326405	-2.931229
34	1	-5.926880	4.896819	-1.923254	78	6	6.460315	0.859979	1.398244
35	6	-4.924138	2.970372	-1.761995	79	1	6.184172	1.516484	2.217756
36	6	-5.481961	2.364732	-2.915833	80	6	7.613634	1.185969	0.609752
37	6	-4.014563	2.204293	-0.996987	81	6	8.394943	2.336717	0.887793
38	6	-5.115984	1.064211	-3.242129	82	6	7.994927	0.354631	-0.482660

39	1	-6.184761	2.916176	-3.531834	83	6	9.497539	2.616343	0.094493
40	1	-5.522650	0.569666	-4.115975	84	1	8.122584	2.984262	1.715701
41	6	-4.198053	0.366955	-2.429544	85	1	10.120347	3.484998	0.273789
42	1	-3.897496	-0.643929	-2.672773	86	6	9.801944	1.735530	-0.970872
43	7	-3.653294	0.920046	-1.331813	87	1	10.659135	1.929749	-1.609038
44	6	-1.528450	-3.564398	-2.355987	88	7	9.083242	0.642359	-1.257218

Table S7 Optimized geometry coordinates of Ru-PSO_2P.

Center	Atomic	Coordinates (Å)			Center	Atomic	Coordinates (Å)		
Number	Number	X	Y	Z	Number	Number	X	Y	Z
1	1	1.373296	1.014409	5.089007	46	6	3.740090	-4.744140	0.307791
2	6	0.924051	0.636289	4.175692	47	7	2.921742	-2.140289	0.288651
3	1	-0.998703	0.267019	5.045703	48	6	3.968513	-3.934417	-0.798396
4	6	-0.392843	0.221227	4.146784	49	6	2.698104	-2.847722	1.321019
5	7	1.183409	0.111306	1.928784	50	6	3.522107	-2.596579	-0.746672
6	6	-0.890549	-0.248950	2.936858	51	6	4.626670	-4.395069	-1.950703
7	6	1.678377	0.558889	3.010823	52	1	2.190344	-2.379187	2.158727
8	6	-0.027056	-0.282735	1.823699	53	6	4.846283	-3.540136	-3.037241
9	6	-2.212843	-0.678865	2.787144	54	1	4.981719	-5.422112	-2.007147
10	1	2.718461	0.875500	3.005942	55	1	5.368291	-3.922478	-3.912056
11	6	-2.677318	-1.132640	1.539397	56	6	4.412442	-2.204766	-2.996800
12	1	-2.875316	-0.651494	3.652017	57	6	4.622894	-1.316517	-4.044899
13	6	-1.822266	-1.211170	0.401912	58	6	3.743791	-1.730895	-1.847812
14	6	-2.165667	-1.687413	-0.876872	59	6	4.169529	-0.020644	-3.885807
15	6	-0.489975	-0.760779	0.565914	60	1	5.140002	-1.613184	-4.951130
16	6	-1.210400	-1.669129	-1.875026	61	1	4.327806	0.722064	-4.660830
17	1	-3.132511	-2.115116	-1.112030	62	6	3.523091	0.327369	-2.704238
18	1	-1.417794	-2.058310	-2.866834	63	1	3.174797	1.343398	-2.544261
19	6	0.049936	-1.183328	-1.575377	64	7	3.334868	-0.519272	-1.774851
20	1	0.834835	-1.175379	-2.327747	65	1	-0.117219	4.334490	-1.322080
21	7	0.335560	-0.768829	-0.411541	66	1	2.891666	-4.763069	2.283175
22	44	2.332941	-0.058461	0.096533	67	1	-9.222253	-2.821032	0.332612
23	6	0.791839	3.934495	-0.889678	68	6	-8.672092	-1.941553	-0.000645
24	1	1.733259	5.851929	-0.637664	69	1	-6.944280	-2.492339	1.074386
25	6	1.819615	4.778040	-0.511599	70	6	-7.364439	-1.735772	0.406427
26	7	2.007620	2.072038	-0.217623	71	7	-8.561177	0.075745	-1.223636
27	6	2.964192	4.198790	0.023534	72	6	-6.620356	-0.607169	-0.010979
28	6	0.946540	2.563151	-0.713387	73	6	-9.249998	-1.011354	-0.827415
29	6	3.001366	2.793696	0.148292	74	6	-7.272441	0.344222	-0.860411
30	6	4.075136	4.954943	0.433333	75	6	-5.274029	-0.357333	0.377710
31	1	0.164095	1.870422	-1.002233	76	1	-10.272450	-1.109955	-1.185707
32	6	5.212695	4.327094	0.954411	77	6	-4.607094	0.805088	-0.016643
33	1	4.067917	6.039303	0.345606	78	1	-3.589567	1.004344	0.323566
34	1	6.061274	4.936577	1.259037	79	6	-5.234431	1.736515	-0.843601
35	6	5.266123	2.928964	1.076868	80	6	-4.535023	2.882170	-1.233593
36	6	6.377999	2.261747	1.577386	81	6	-6.573394	1.523753	-1.286675
37	6	4.154574	2.158673	0.674010	82	6	-5.136729	3.818304	-2.056698
38	6	6.321387	0.882166	1.639660	83	1	-3.508693	3.060044	-0.901410
39	1	7.267659	2.791242	1.901022	84	1	-4.595723	4.712862	-2.364190
40	1	7.163770	0.306415	2.009618	85	6	-6.430739	3.594556	-2.477893
41	6	5.167544	0.234303	1.210755	86	1	-6.957149	4.292326	-3.125885
42	1	5.100408	-0.849800	1.240278	87	7	-7.100826	2.486950	-2.095839
43	7	4.166626	0.882818	0.770236	88	16	-4.403808	-1.541434	1.428083
44	6	3.090834	-4.180391	1.389676	89	8	-4.522096	-2.814081	0.747265
45	1	4.061335	-5.779852	0.335396	90	8	-5.018998	-1.324290	2.722586

Table S8 Optimized geometry coordinates of Re-PSP.

Center	Atomic	Coordinates (Å)			Center	Atomic	Coordinates (Å)		
Number	Number	X	Y	Z	Number	Number	X	Y	Z
1	1	5.132378	5.078514	-0.376133	27	7	-1.734135	-0.169819	1.310546
2	6	5.313144	4.009749	-0.335043	28	6	0.507291	-0.833614	1.602004
3	1	3.615386	3.573558	0.903951	29	6	-1.810148	0.234835	2.513714
4	6	4.472944	3.173451	0.373918	30	6	-0.663836	-0.677391	0.812866
5	7	6.628540	2.209163	-0.984747	31	6	1.666227	-1.393130	0.999705
6	6	4.763982	1.813917	0.367412	32	1	-2.738914	0.679632	2.854779
7	6	6.396608	3.458470	-1.009619	33	6	1.643669	-1.798640	-0.343822
8	6	5.890688	1.374858	-0.354894	34	1	2.534620	-2.234698	-0.791605
9	6	3.977861	0.873118	1.045716	35	6	0.491743	-1.642888	-1.122342
10	1	7.070234	4.089158	-1.582685	36	6	0.459264	-2.030921	-2.453998
11	6	4.292220	-0.497776	1.007242	37	6	-0.670610	-1.077961	-0.548902
12	1	3.107230	1.213618	1.603518	38	6	-0.720151	-1.838213	-3.139544
13	6	5.431420	-0.958706	0.290124	39	1	1.321196	-2.465030	-2.948242
14	6	5.839395	-2.297244	0.199290	40	1	-0.807197	-2.116007	-4.184489
15	6	6.223424	-0.005832	-0.393459	41	6	-1.801622	-1.275368	-2.472440
16	6	6.968803	-2.596895	-0.537535	42	1	-2.731102	-1.119851	-3.009248
17	1	5.302121	-3.098736	0.694573	43	7	-1.738415	-0.932182	-1.247225
18	1	7.325013	-3.617462	-0.625861	44	75	-3.416866	-0.035633	-0.113131
19	6	7.649845	-1.562362	-1.158899	45	6	-3.834845	-2.140349	0.364781
20	1	8.545901	-1.760853	-1.739857	46	8	-4.059835	-3.240229	0.614382
21	7	7.256018	-0.359413	-1.064539	47	6	-4.713335	0.304468	-1.843653
22	16	3.208301	-1.624541	1.905329	48	8	-5.396750	0.478411	-2.752061
23	1	-0.836090	0.485958	4.412195	49	6	-4.980576	0.671437	1.251501
24	6	-0.742808	0.134221	3.390543	50	8	-5.801705	1.038946	1.967794
25	1	1.279831	-0.493197	3.613281	51	35	-2.826771	2.312602	-0.405733
26	6	0.437866	-0.411538	2.934817					

Table S9 Optimized geometry coordinates of Re-PSO_2P.

Center	Atomic	Coordinates (Å)			Center	Atomic	Coordinates (Å)		
Number	Number	X	Y	Z	Number	Number	X	Y	Z
1	1	9.296633	-0.154782	-2.693454	28	6	-2.071640	1.554930	1.913820
2	6	8.515449	-0.365612	-1.963468	29	6	-0.803619	0.752360	0.246888
3	1	7.374375	1.365961	-2.475539	30	6	1.509846	1.372162	-0.140289
4	6	7.429592	0.482465	-1.833679	31	1	-3.041971	1.572596	2.401416
5	7	7.621714	-1.733078	-0.241691	32	6	1.541607	0.561738	-1.290669
6	6	6.432920	0.208252	-0.893145	33	1	2.429750	0.521529	-1.916442
7	6	8.589015	-1.474660	-1.147379	34	6	0.418870	-0.179724	-1.667593
8	6	6.522869	-0.944829	-0.060991	35	6	0.418155	-0.996183	-2.791154
9	6	5.355280	1.081858	-0.768205	36	6	-0.755951	-0.097137	-0.889742
10	1	9.419471	-2.175827	-1.198239	37	6	-0.742725	-1.686965	-3.068633
11	6	4.341702	0.840848	0.166923	38	1	1.273442	-1.084303	-3.450779
12	1	5.312964	1.979388	-1.393255	39	1	-0.819872	-2.325886	-3.943150
13	6	4.371162	-0.297936	1.016617	40	6	-1.838256	-1.530344	-2.226532
14	6	3.380344	-0.595176	1.981190	41	1	-2.764189	-2.050037	-2.455848
15	6	5.481105	-1.200127	0.896783	42	7	-1.799469	-0.767107	-1.207683
16	6	3.460183	-1.719056	2.786897	43	75	-3.473427	-0.436854	0.095930
17	1	2.516168	0.049563	2.149433	44	6	-2.998284	-2.114814	1.378613
18	1	2.686176	-1.924930	3.525947	45	8	-2.740116	-3.005237	2.059082
19	6	4.538939	-2.554337	2.636950	46	6	-4.993504	-1.668374	-0.843458
20	1	4.666389	-3.450911	3.239890	47	8	-5.794835	-2.326839	-1.339637
21	7	5.493386	-2.284704	1.726495	48	6	-5.117519	0.035227	1.432502
22	1	-1.241110	3.030076	3.233279	49	8	-5.985019	0.281832	2.145594
23	6	-1.062021	2.374836	2.386097	50	35	-4.066004	1.427769	-1.333702
24	1	0.916717	3.052673	2.093295	51	16	3.058141	2.119929	0.317612
25	6	0.155874	2.367330	1.738313	52	8	3.101657	2.429580	1.731144
26	7	-1.905655	0.807053	0.899279	53	8	3.362242	3.115223	-0.687828
27	6	0.327391	1.519357	0.634146					

Table S10 Optimized geometry coordinates of Re-PSP-Re.

Center	Atomic	Coordinates (Å)			Center	Atomic	Coordinates (Å)		
Number	Number	X	Y	Z	Number	Number	X	Y	Z
1	1	-1.230796	2.479397	-2.930004	49	6	-4.046571	-2.142102	-2.073389
2	6	-1.411507	1.826318	-2.084791	50	6	-6.062794	-2.464564	-0.936425
3	1	0.666874	1.588159	-1.557768	51	6	-7.498178	-4.429934	-1.256516
4	6	-0.360684	1.331706	-1.322139	52	1	-3.181447	-1.517442	-2.254636
5	7	-3.035480	0.670426	-0.730652	53	6	-8.399469	-3.939693	-0.345525
6	6	-0.647966	0.479701	-0.225910	54	1	-7.677219	-5.378936	-1.752334
7	6	-2.740259	1.477888	-1.764776	55	1	-9.302101	-4.495135	-0.110366
8	6	-2.002678	0.180525	0.031722	56	6	-8.171774	-2.683975	0.320635
9	6	0.363015	-0.092068	0.616618	57	6	-9.059161	-2.124590	1.273972
10	1	-3.568979	1.849486	-2.353014	58	6	-6.996656	-1.958307	0.017330
11	6	0.035390	-0.916207	1.663464	59	6	-8.741106	-0.906449	1.862645
12	1	1.397270	0.152344	0.398960	60	1	-9.972917	-2.647801	1.536144
13	6	-1.349477	-1.233386	1.953468	61	1	-9.395814	-0.449638	2.594892
14	6	-1.781111	-2.068199	3.014565	62	6	-7.546246	-0.245462	1.509535
15	6	-2.349426	-0.670179	1.124299	63	1	-7.279988	0.700209	1.963568
16	6	-3.139823	-2.297292	3.193619	64	7	-6.687454	-0.756062	0.609829
17	1	-1.064963	-2.525503	3.688776	65	1	-4.347173	3.568721	3.789903
18	1	-3.497524	-2.930795	3.995994	66	1	-3.446470	-3.680173	-3.456857
19	6	-4.073703	-1.698300	2.327231	67	16	1.288091	-1.690253	2.757947
20	1	-5.135991	-1.859329	2.455553	68	1	4.018789	-4.078200	-0.971941
21	7	-3.692097	-0.898538	1.316358	69	6	4.225372	-3.158396	-0.439020
22	44	-4.902861	0.057967	-0.071561	70	1	2.436627	-3.208629	0.762817
23	6	-4.764706	3.389202	2.806546	71	6	3.348861	-2.673554	0.522470
24	1	-5.628340	5.353678	2.581630	72	7	5.720314	-1.301719	-0.108948
25	6	-5.474652	4.377084	2.134426	73	6	3.657831	-1.467439	1.198195
26	7	-5.072900	1.832787	0.991916	74	6	5.405558	-2.449030	-0.733840
27	6	-6.001908	4.095567	0.849072	75	6	4.864094	-0.813682	0.846349
28	6	-4.580533	2.125446	2.208221	76	6	2.826182	-0.859506	2.214037
29	6	-5.770942	2.806329	0.316077	77	1	6.097440	-2.813230	-1.481425
30	6	-6.754496	5.041290	0.066899	78	6	3.202434	0.302657	2.837470
31	1	-4.036132	1.343089	2.720807	79	1	2.574059	0.737622	3.607817
32	6	-7.241013	4.705809	-1.171415	80	6	4.426341	0.968636	2.488678
33	1	-6.931667	6.030005	0.478770	81	6	4.857659	2.170257	3.102019
34	1	-7.809578	5.424906	-1.752796	82	6	5.247641	0.403542	1.488897
35	6	-7.010214	3.399332	-1.730290	83	6	6.059786	2.736927	2.698924
36	6	-7.479819	2.991935	-3.004223	84	1	4.253076	2.634638	3.873909
37	6	-6.270401	2.459999	-0.975474	85	1	6.426754	3.654007	3.142708
38	6	-7.196852	1.706549	-3.450798	86	6	6.823803	2.113811	1.691655
39	1	-8.051033	3.681251	-3.617529	87	1	7.761427	2.544460	1.366225
40	1	-7.539482	1.360720	-4.418612	88	7	6.431189	0.974049	1.095180
41	6	-6.449194	0.828381	-2.638937	89	75	7.442911	-0.064425	-0.497667
42	1	-6.215043	-0.173714	-2.974149	90	6	8.548526	-1.036174	0.687919
43	7	-5.990423	1.191771	-1.428536	91	8	9.255570	-1.651991	1.435256
44	6	-4.207365	-3.368204	-2.751663	92	6	8.815529	1.234598	-0.779538
45	1	-5.470556	-5.095953	-3.026287	93	8	9.662524	2.064847	-0.957920
46	6	-5.329928	-4.151468	-2.510852	94	6	8.100126	-1.058068	-1.991809
47	7	-4.951943	-1.692885	-1.186663	95	8	8.493247	-1.681029	-2.938375
48	6	-6.298657	-3.702069	-1.578708	96	35	5.774760	1.308933	-2.113737

Table S11 Optimized geometry coordinates of Re-PSO_2P-Re.

Center	Atomic	Coordinates (Å)			Center	Atomic	Coordinates (Å)		
Number	Number	X	Y	Z	Number	Number	X	Y	Z
1	1	-4.866758	_-0.515302	-5.154166	50	6	-5.953774	-1.846542	1.879240
2	6	-4.261371	-0.692521	-4.272355	51	6	-6.964788	-2.968603	3.795332
3	1	-2.627385	-1.595863	-5.337746	52	1	-5.302538	-2.771659	-1.157906
4	6	-3.014923	-1.292956	-4.371033	53	6	-6.799389	-1.819574	4.565192
5	7	-4.030334	-0.504402	-1.943459	54	1	-7.421117	-3.846369	4.245824
6	6	-2.281075	-1.484632	-3.194507	55	1	-7.131409	-1.823931	5.600228
7	6	-4.731680	-0.306822	-3.013656	56	6	-6.208616	-0.657876	4.013435
8	6	-2.853187	-1.063173	-1.974110	57	6	-6.020959	0.524024	4.741171
9	6	-0.998157	-2.066141	-3.183666	58	6	-5.784496	-0.676042	2.664029
10	1	-5.700116	0.171607	-2.910336	59	6	-5.435900	1.605798	4.097432
11	6	-0.303127	-2.221703	-1.984491	60	1	-6.326966	0.603127	5.778323
12	1	-0.546139	-2.383502	-4.121587	61	1	-5.278389	2.544447	4.616767
13	6	-0.862277	-1.835475	-0.727121	62	6	-5.054233	1.477357	2.757877
14	6	-0.257128	-1.980725	0.538936	63	1	-4.602586	2.310287	2.229068
15	6	-2.149490	-1.240617	-0.748488	64	7	-5.232848	0.370051	2.112105
16	6	-0.931393	-1.534531	1.665571	65	1	-1.405894	4.109040	-0.590109
17	1	0.712100	-2.448113	0.673801	66	1	-6.320024	-4.899352	-0.353760
18	1	-0.497309	-1.642234	2.653140	67	1	6.022933	-4.460079	-0.314065
19	6	-2.188964	-0.954038	1.513159	68	6	5.576824	-3.473050	-0.356786
20	1	-2.742906	-0.601768	2.377134	69	1	3.804511	-4.150673	-1.318776
21	7	-2.729226	-0.829516	0.345784	70	6	4.322964	-3.287855	-0.916290
22	44	-4.680372	0.063110	0.039610	71	7	5.761577	-1.178046	0.093888
23	6	-2.441688	3.796014	-0.657589	72	6	3.783403	-1.988120	-0.966771
24	1	-3.178543	5.709916	-1.305790	73	6	6.265922	-2.369702	0.142580
25	6	-3.430361	4.685312	-1.055870	74	6	4.592096	-0.943239	-0.444094
26	7	-4.023681	2.078586	-0.415551	75	6	2.515934	-1.627647	-1.514630
27	6	-4.750242	4.221593	-1.125017	76	1	7.251912	-2.504401	0.572289
28	6	-2.795381	2.479754	-0.343374	77	6	2.107101	-0.295793	-1.598659
29	6	-4.993528	2.870521	-0.783607	78	1	1.160217	-0.031156	-2.062119
30	6	-5.837112	5.039305	-1.516362	79	6	2.920319	0.736101	-1.091609
31	1	-2.042085	1.764052	-0.031555	80	6	2.545492	2.082007	-1.151459
32	6	-7.132011	4.528004	-1.563945	81	6	4.161094	0.409165	-0.499710
33	1	-5.669100	6.079553	-1.783245	82	6	3.421252	3.020826	-0.630577
34	1	-7.947702	5.179874	-1.866106	83	1	1.607616	2.393461	-1.597718
35	6	-7.390378	3.179137	-1.222146	84	1	3.186557	4.078705	-0.664041
36	6	-8.672410	2.615654	-1.247635	85	6	4.625455	2.590854	-0.064736
37	6	-6.312970	2.349669	-0.832061	86	1	5.320237	3.322138	0.332411
38	6	-8.811303	1.282723	-0.885587	87	7	4.942632	1.334364	-0.007898
39	1	-9.540112	3.198869	-1.534961	88	75	6.745499	0.572108	0.857316
40	1	-9.784614	0.804928	-0.881360	89	6	5.852972	0.356370	2.770872
41	6	-7.675671	0.554574	-0.515763	90	8	5.377229	0.243127	3.823671
42	1	-7.757466	-0.486835	-0.221896	91	6	7.635852	2.369445	1.554242
43	7	-6.501701	1.099389	-0.509537	92	8	8.124538	3.346972	1.942007
44	6	-6.238449	-4.049752	0.314988	93	6	8.510783	-0.290699	1.664293
45	1	-7.130833	-5.044952	1.999446	94	8	9.473998	-0.755511	2.112396
46	6	-6.687802	-4.128528	1.625959	95	35	7.815825	0.835345	-1.337246
47	7	-5.552832	-1.827873	0.637376	96	16	1.369032	-2.890460	-2.098091
48	6	-6.546160	-3.000442	2.443764	97	8	1.409929	-4.054047	-1.165257
49	6	-5.667197	-2.856638	-0.139568	98	8	1.674949	-3.088161	-3.544990

Photocatalysis

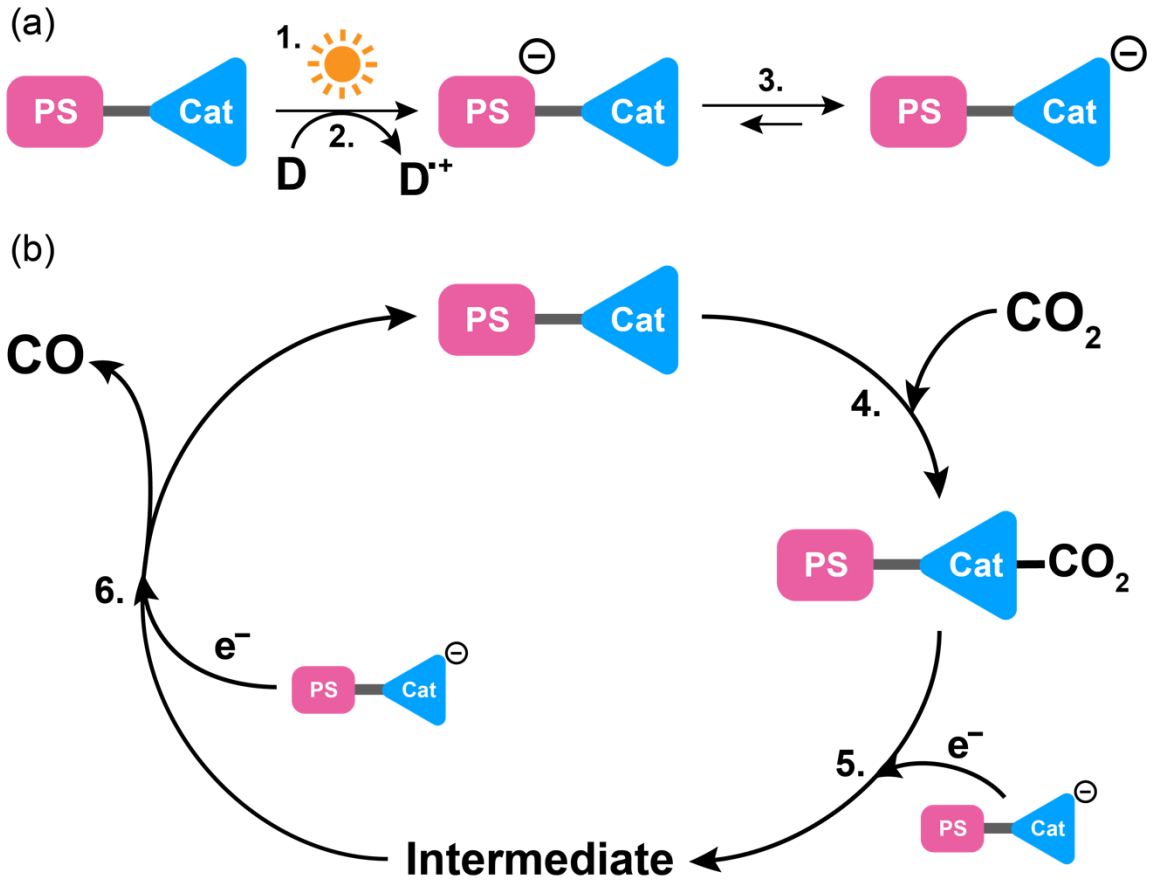

Fig. S7 Depiction of a supramolecular photocatalyst assembly for CO_2 reduction, where (a) illustrates the generation of the one electron reduced species (OERS) of the photocatalyst, and (b) illustrates the catalytic cycle

Photocatalytic reduction is a technique in which CO_2 is converted into useful higher-energy components such as CO or formic acid, and various metal complexes have been reported which are catalytically active for this process. Photochemical CO_2 reduction involves two components: a redox photosensitizer (PS) that absorbs light in the visible region; and a catalytic center at which the reduction occurs. The reaction mechanism can be broken into two sections, the first being the generation of the one electron reduced species (OERS) of the photocatalyst (Fig. S7a), and the second being the catalytic cycle for the production of CO (Fig. S7b). The mechanism proceeds as follows:[15]

1. Irradiation of the metallic PS gives the ^{3}MLCT excited-state.
2. The excited PS unit is quenched by a sacrificial electron donor (D), generating the one electron reduced species (OERS) of the PS.
3. A rapid intramolecular electron transfer from the OERS of the PS to the catalytic center (Cat).
4. CO_2 binds to the photocatalyst.

5. Additional OERS of the PS–Cat remaining in solution functions as a redox photosensitizer and supplies an electron, forming an intermediate.
6. The electron for the second reduction process is supplied again by remaining OERS of PS-Cat, resulting in the formation of CO and the regeneration of PS–Cat.

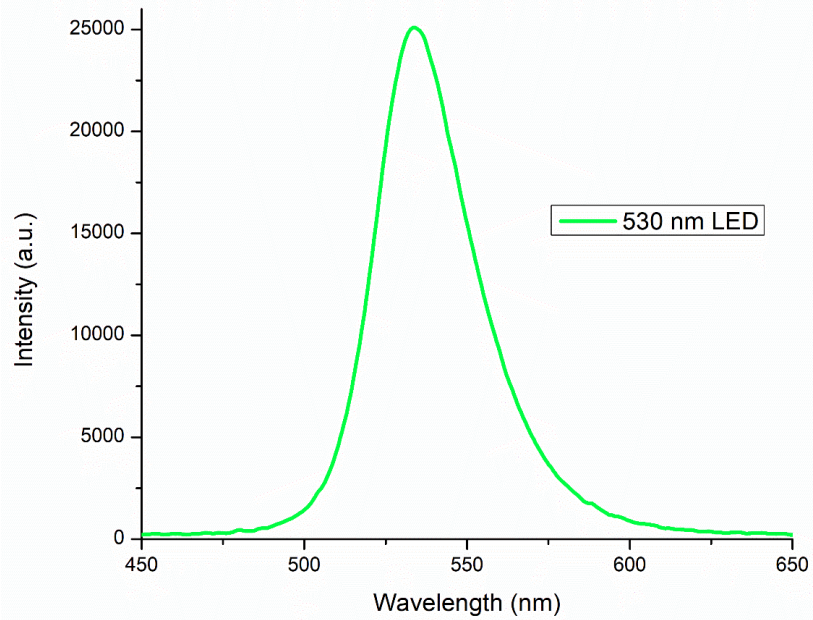

Fig. S8 Emission profile of the green LED used in photocatalytic experiments (λ_{max} = 530 nm, 30 mW, FWHM = 35 nm).

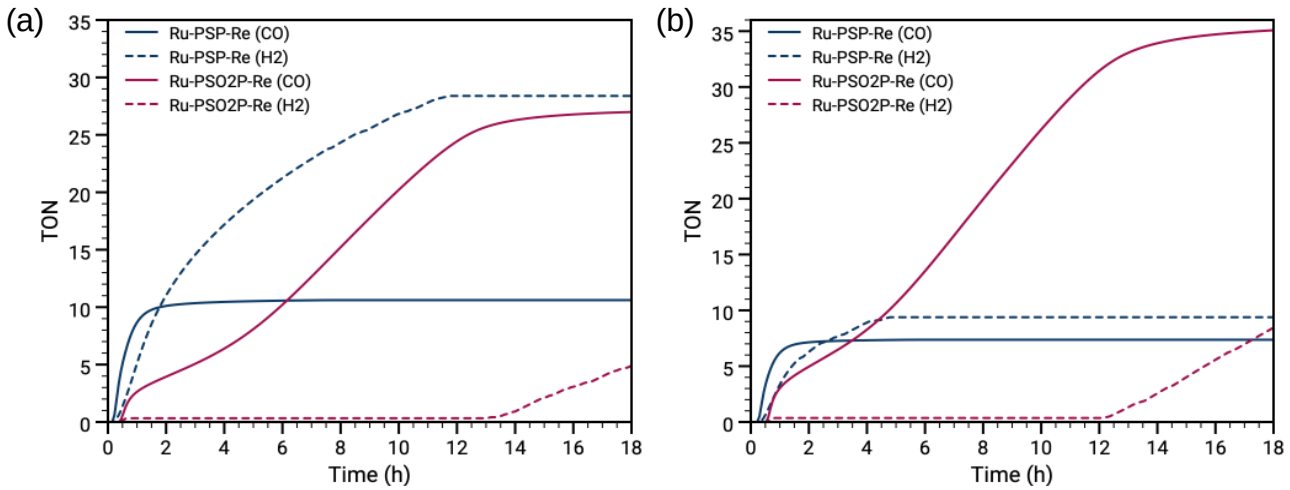

Fig. S9 Photoactivity profile of the dyads showing both CO (plain) and H_2 (dashed) evolution in DMF/TEOA 5:1 with 0.1 M BIH and 0.05 mM of photoactive species under irradiation with a 530 nm LED (30 mW). (a) Run 1. (b) Run 2.

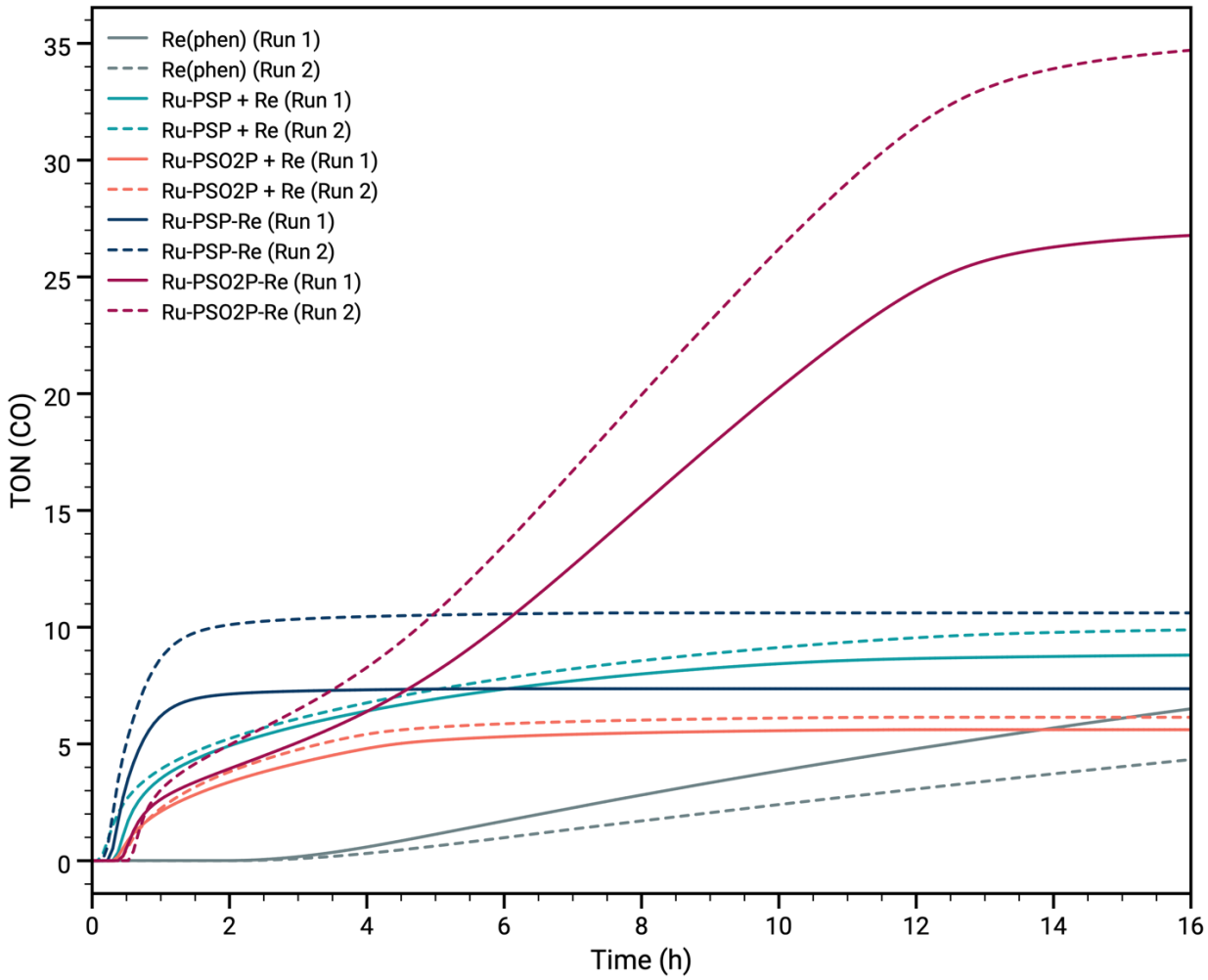

Fig. S10 Reproducibility of the photocatalytic activity. Each curve is based on a fresh solution of DMF/TEOA 5:1 with 0.1 M BIH and 0.05 mM of photoactive species under irradiation with a 530 nm LED (30 mW).

NMR Spectra

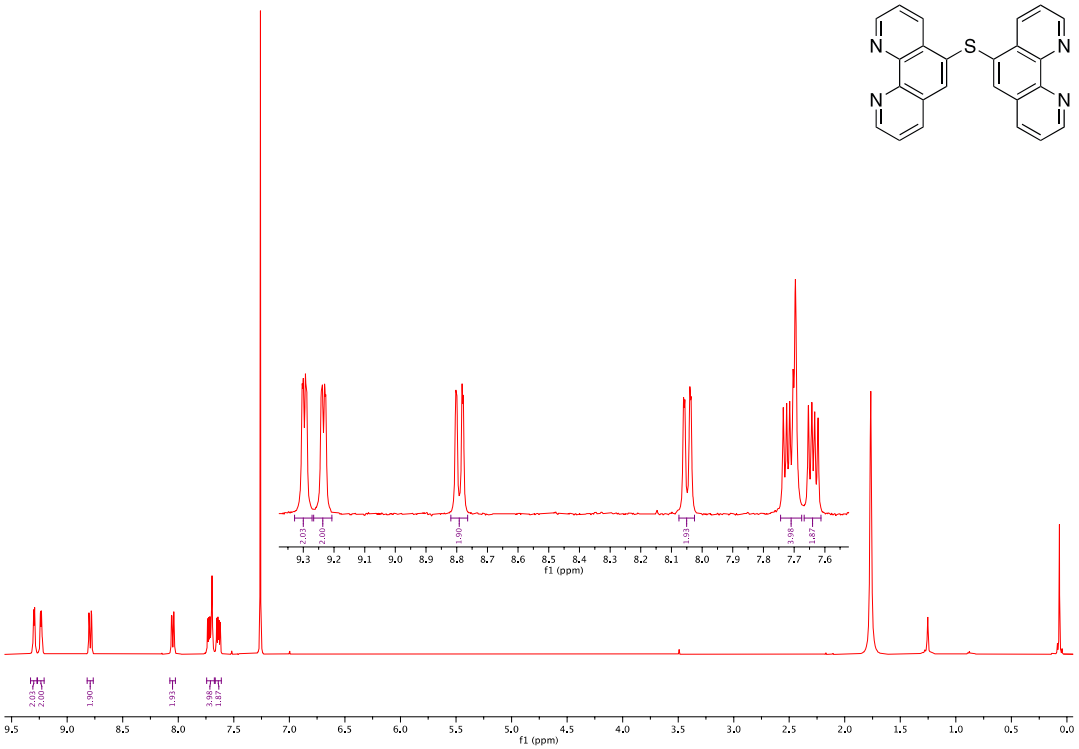

Fig. S11 ^{1}H NMR of **PSP** ($CDCl_3$, 400 MHz, 25 °C).

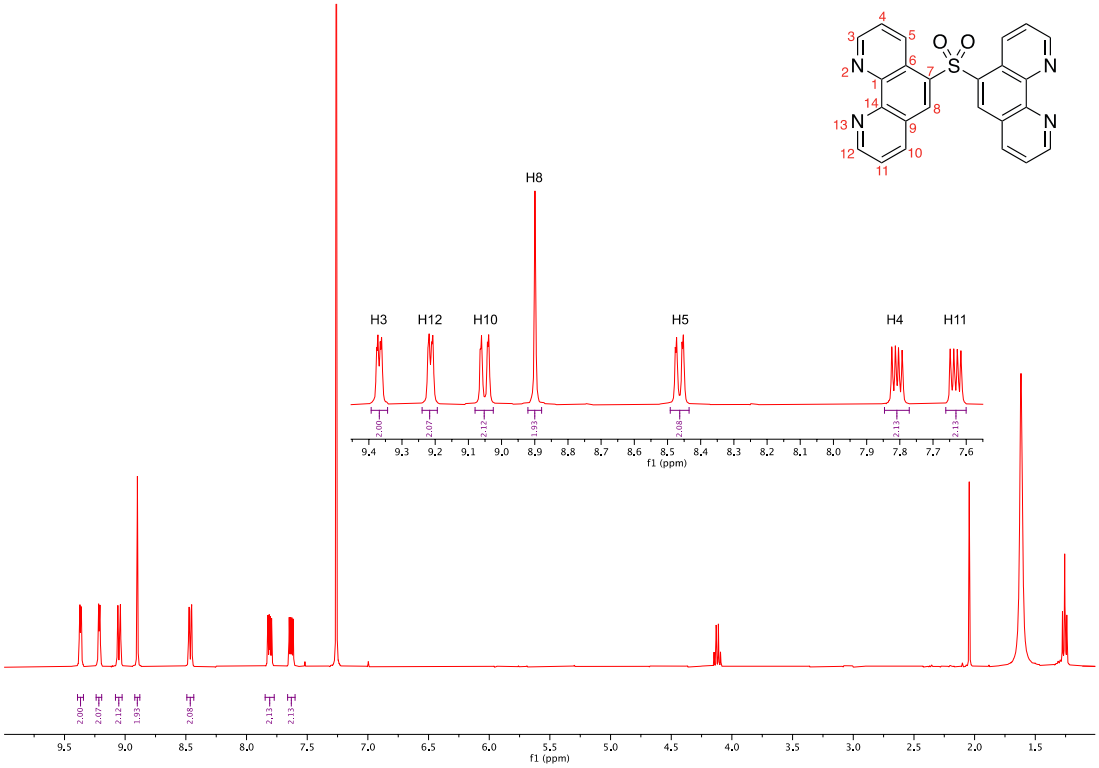

Fig. S12 ^{1}H NMR of **PSO_2P** ($CDCl_3$, 400 MHz, 25 °C).

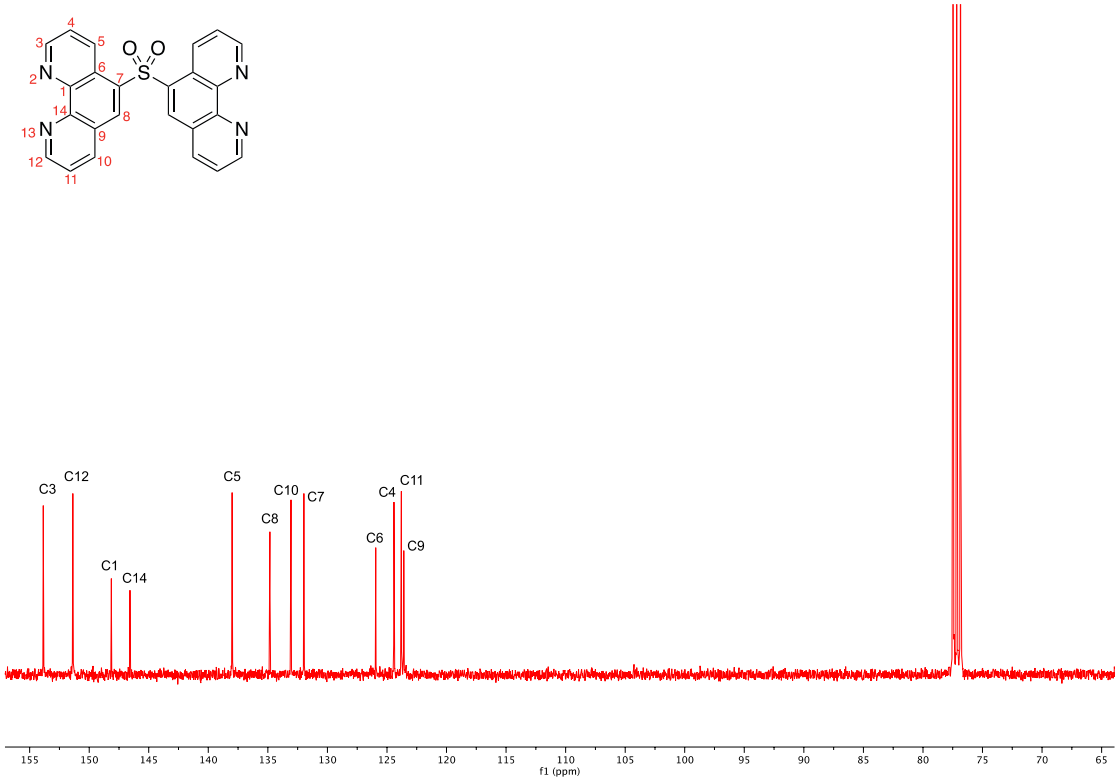

Fig. S13 $^{13}C\{^{1}H\}$ NMR of **PSO_2P** ($CDCl_3$, 101 MHz, 25 °C).

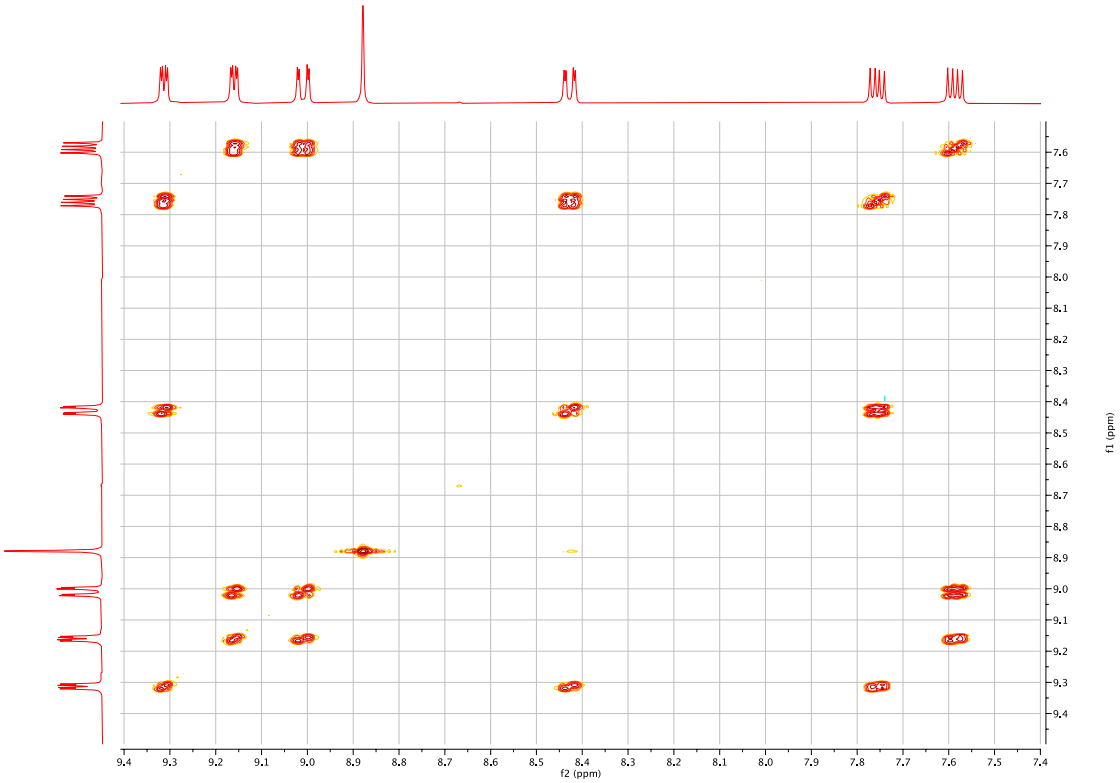

Fig. S14 COSY NMR of **PSO_2P** ($CDCl_3$, 101 MHz, 25 °C).

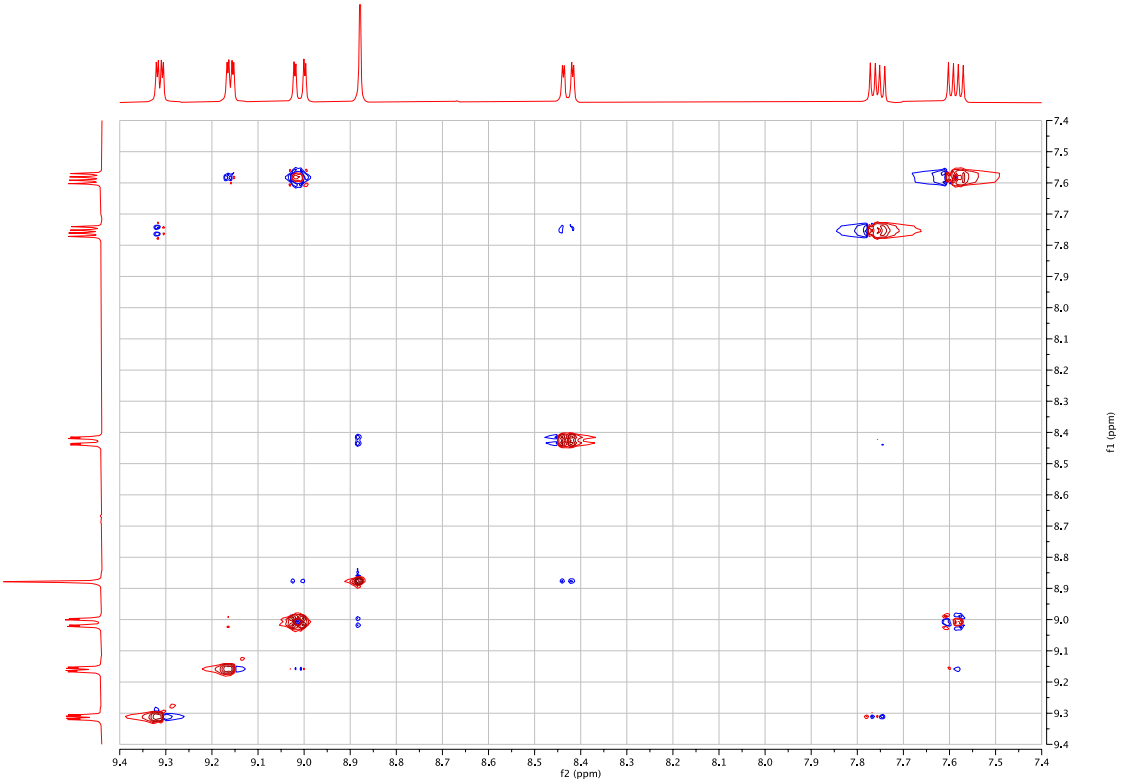

Fig. S15 NOESY NMR of **PSO_2P** ($CDCl_3$, 101 MHz, 25 °C).

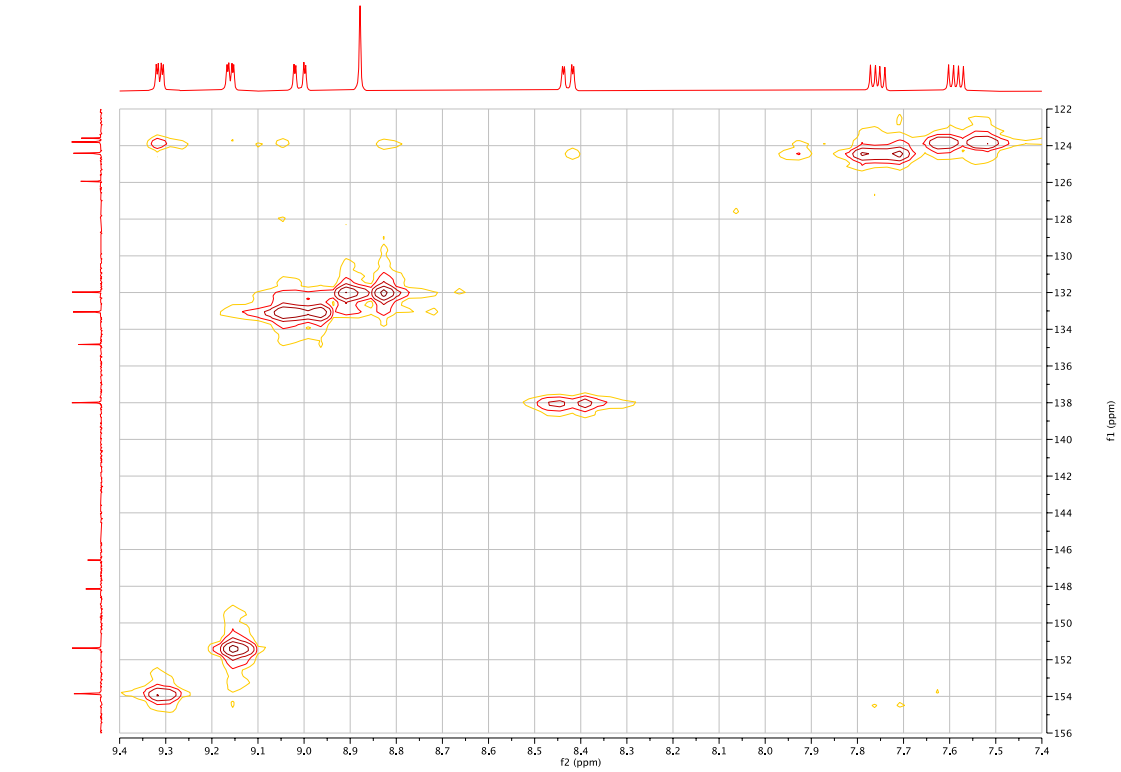

Fig. S16 HSQC NMR of **PSO_2P** ($CDCl_3$, 101 MHz, 25 °C).

Fig. S17 HMBC NMR of **PSO_2P** ($CDCl_3$, 101 MHz, 25 °C).

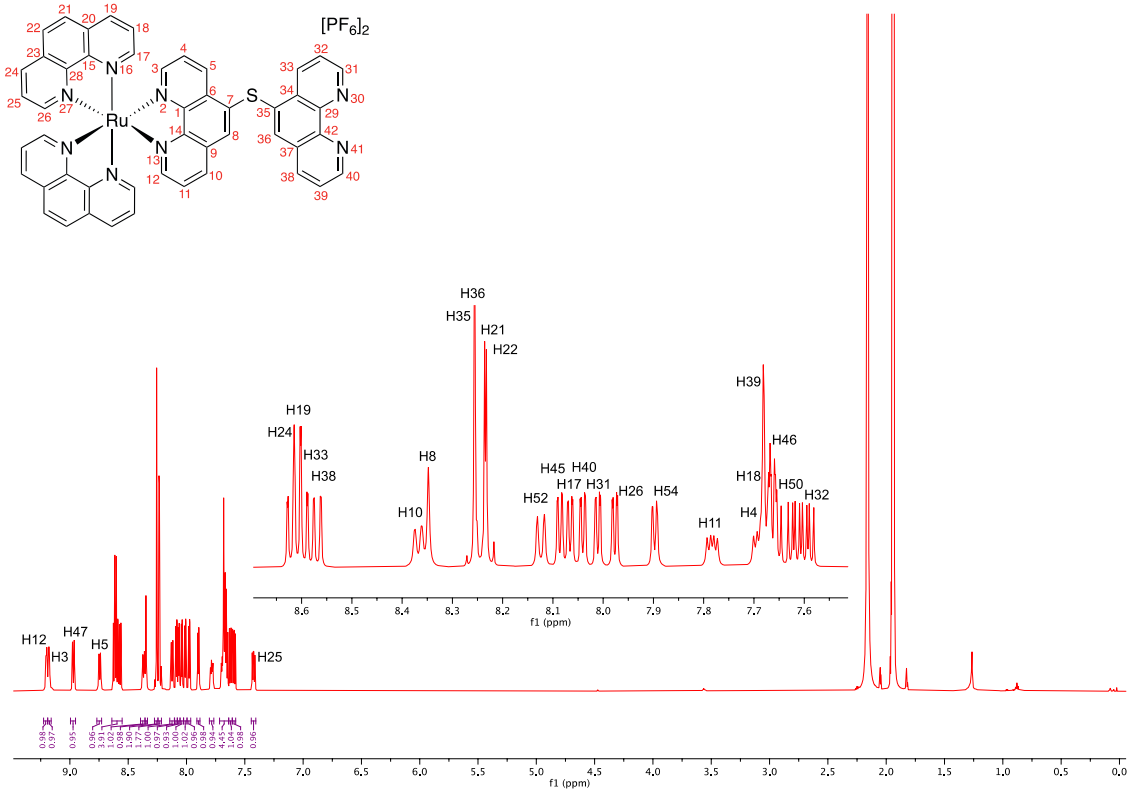

Fig. S18 ^{1}H NMR of **Ru-PSP** (CD_3CN, 600 MHz, 25 °C).

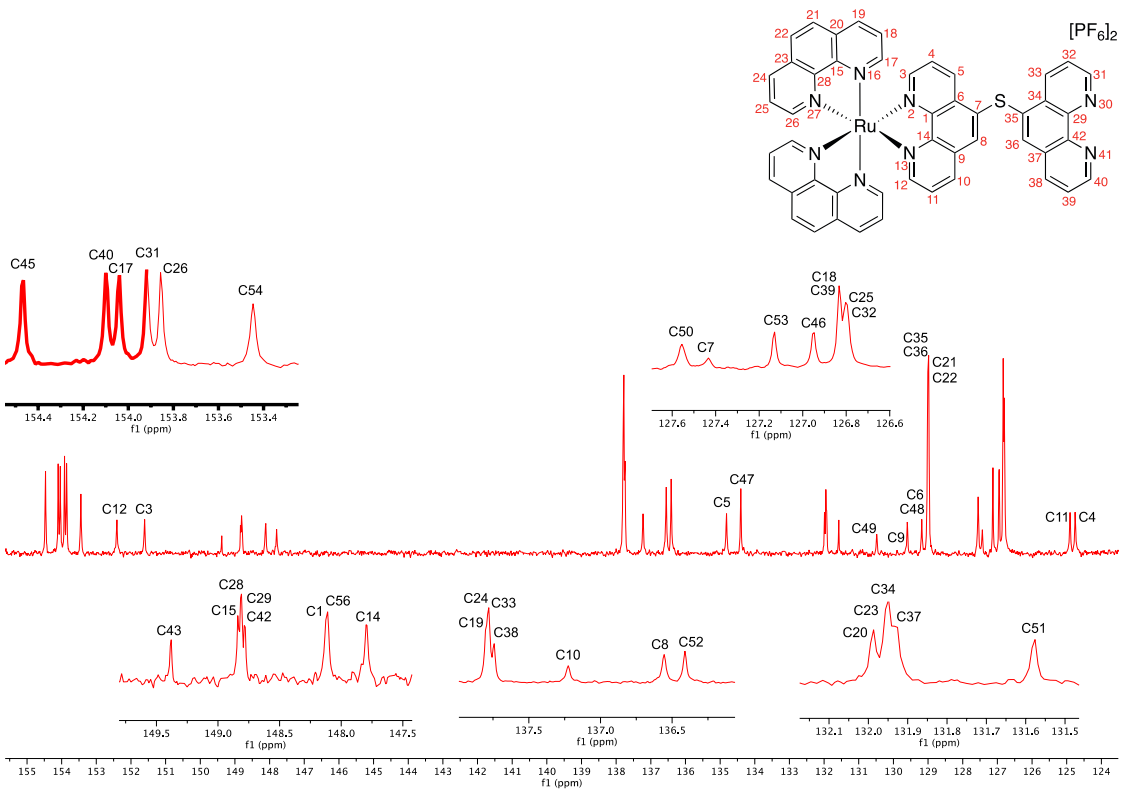

Fig. S19 $^{13}C\{^{1}H\}$ NMR of **Ru-PSP** (CD_3CN, 151 MHz, 25 °C).

Fig. S20 COSY NMR of **Ru-PSP** (CD_3CN, 600 MHz, 25 °C).

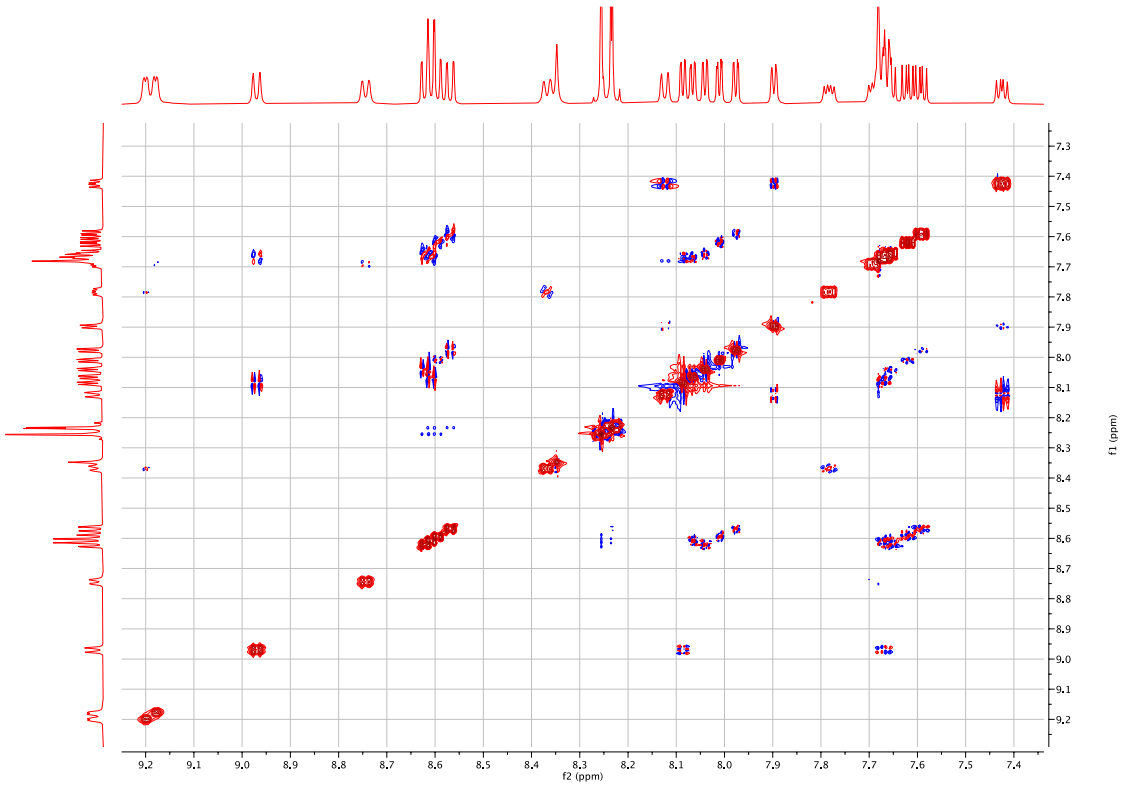

Fig. S21 ROESY NMR of **Ru-PSP** (CD_3CN, 600 MHz, 25 °C).

Fig. S22 HSQC NMR of **Ru-PSP** (CD_3CN, 600 MHz, 25 °C).

Fig. S23 HMBC NMR of **Ru-PSP** (CD_3CN, 600 MHz, 25 °C).

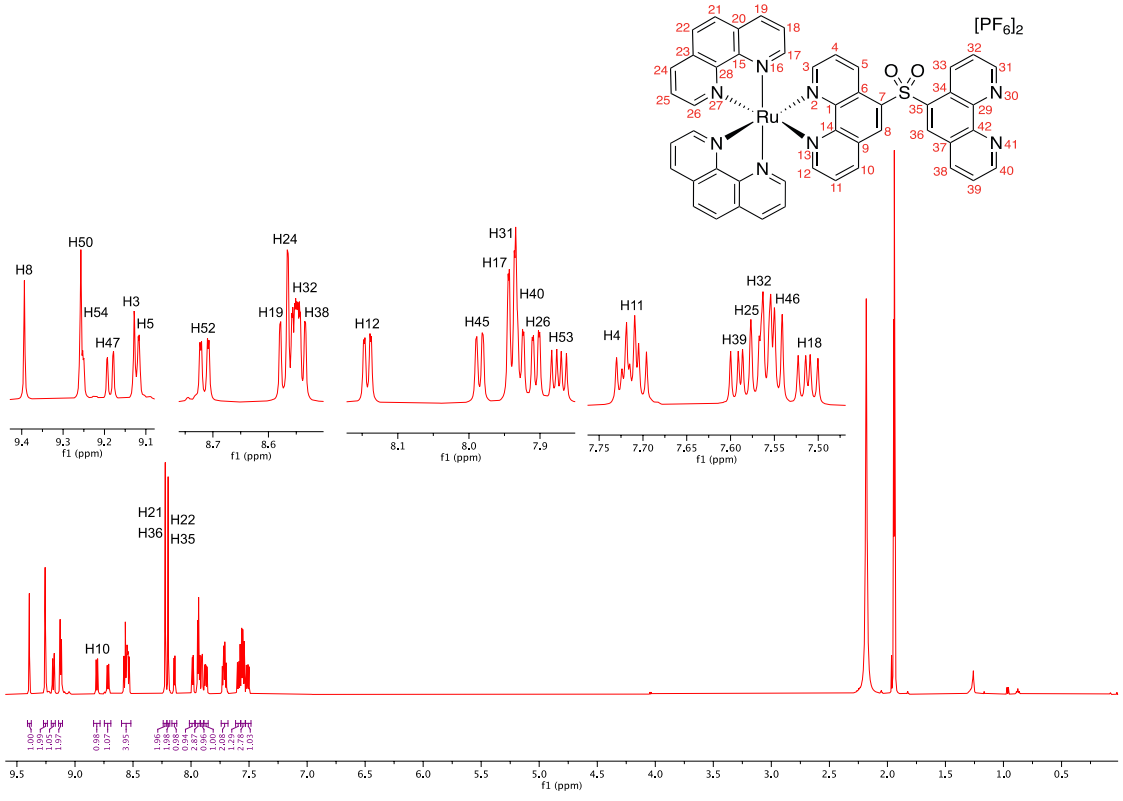

Fig. S24 ^{1}H NMR of **Ru-PSO$_2$P** (CD_3CN, 600 MHz, 25 °C).

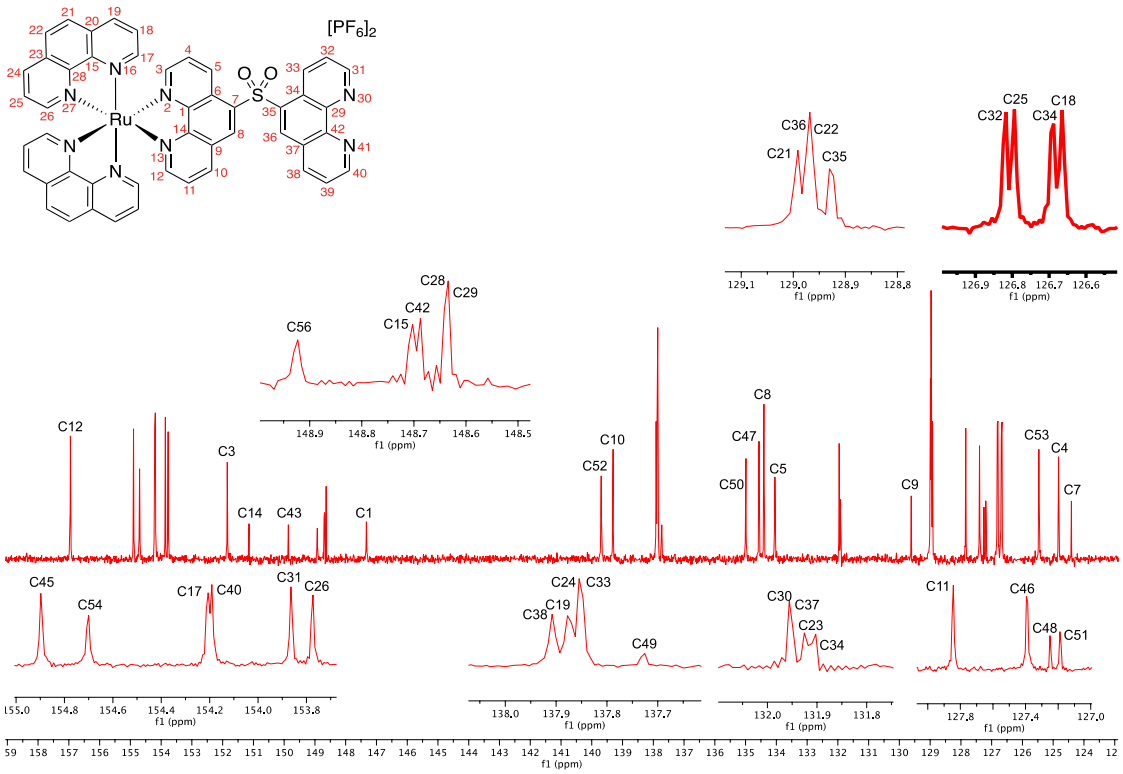

Fig. S25 $^{13}C\{^{1}H\}$ NMR of **Ru-PSO$_2$P** (CD_3CN, 151 MHz, 25 °C).

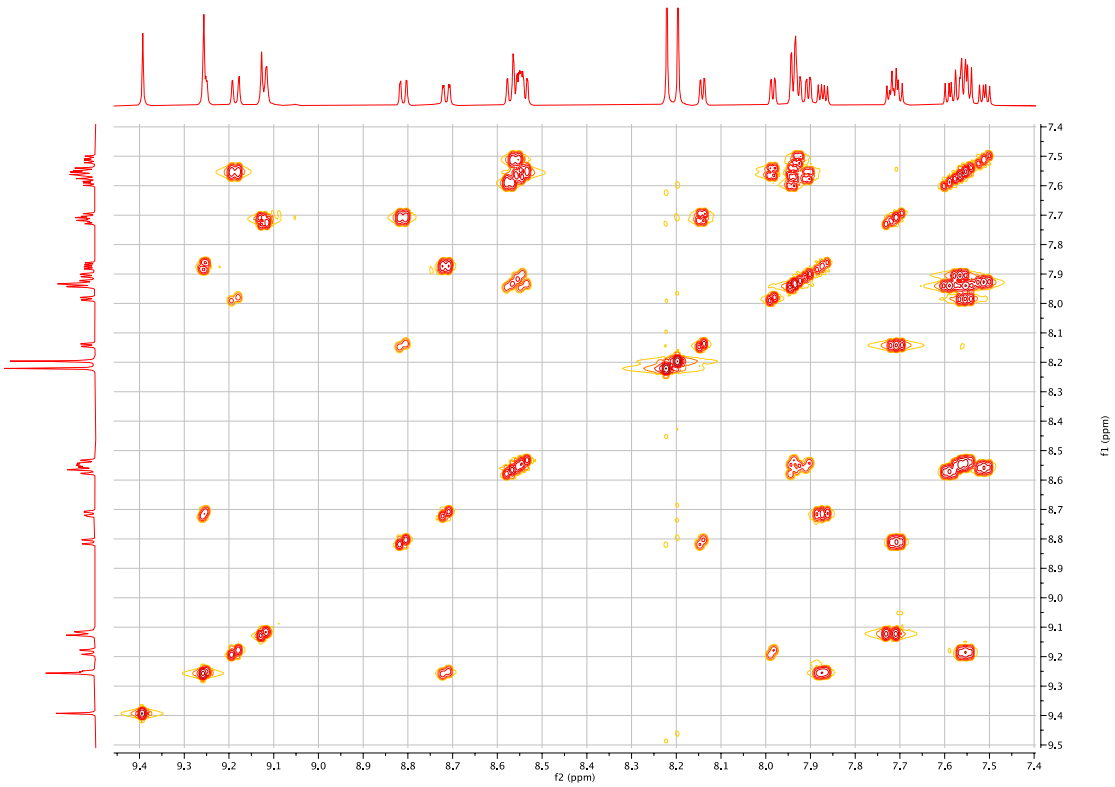

Fig. S26 COSY NMR of **Ru-PSO$_2$P** (CD_3CN, 600 MHz, 25 °C).

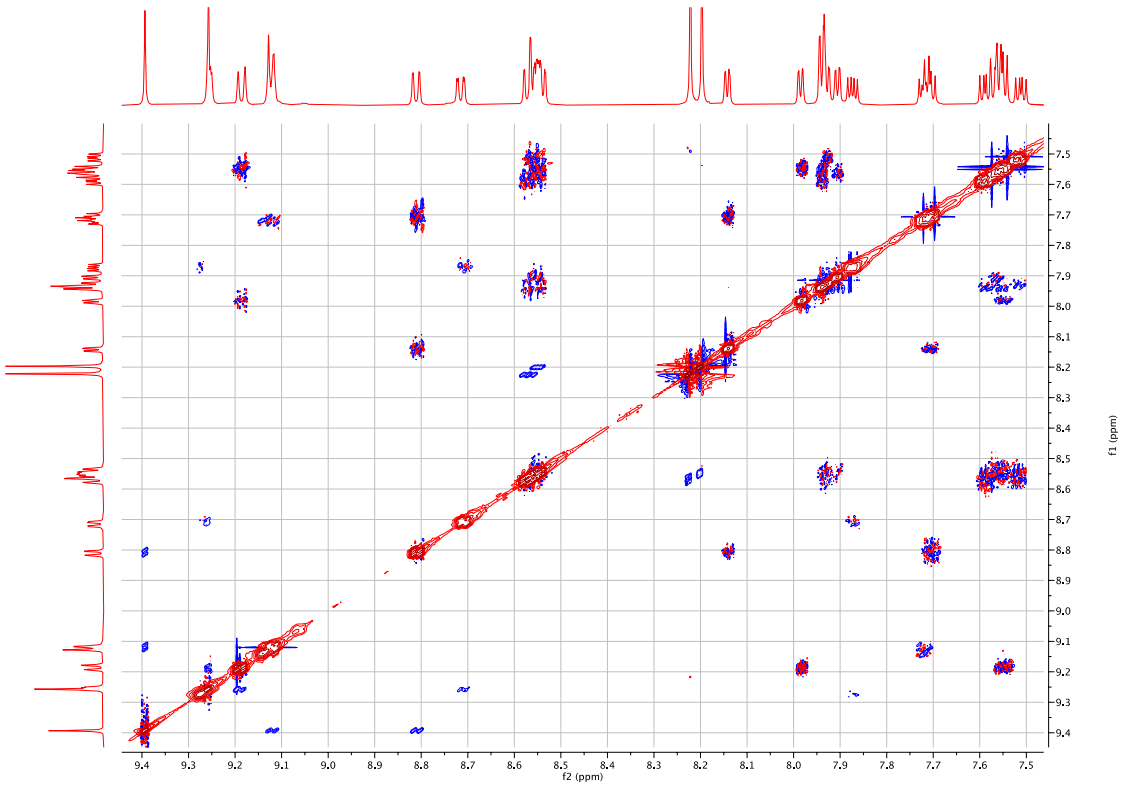

Fig. S27 ROESY NMR of **Ru-PSO$_2$P** (CD_3CN, 600 MHz, 25 °C).

Fig. S28 HSQC NMR of **Ru-PSO$_2$P** (CD_3CN, 600 MHz, 25 °C).

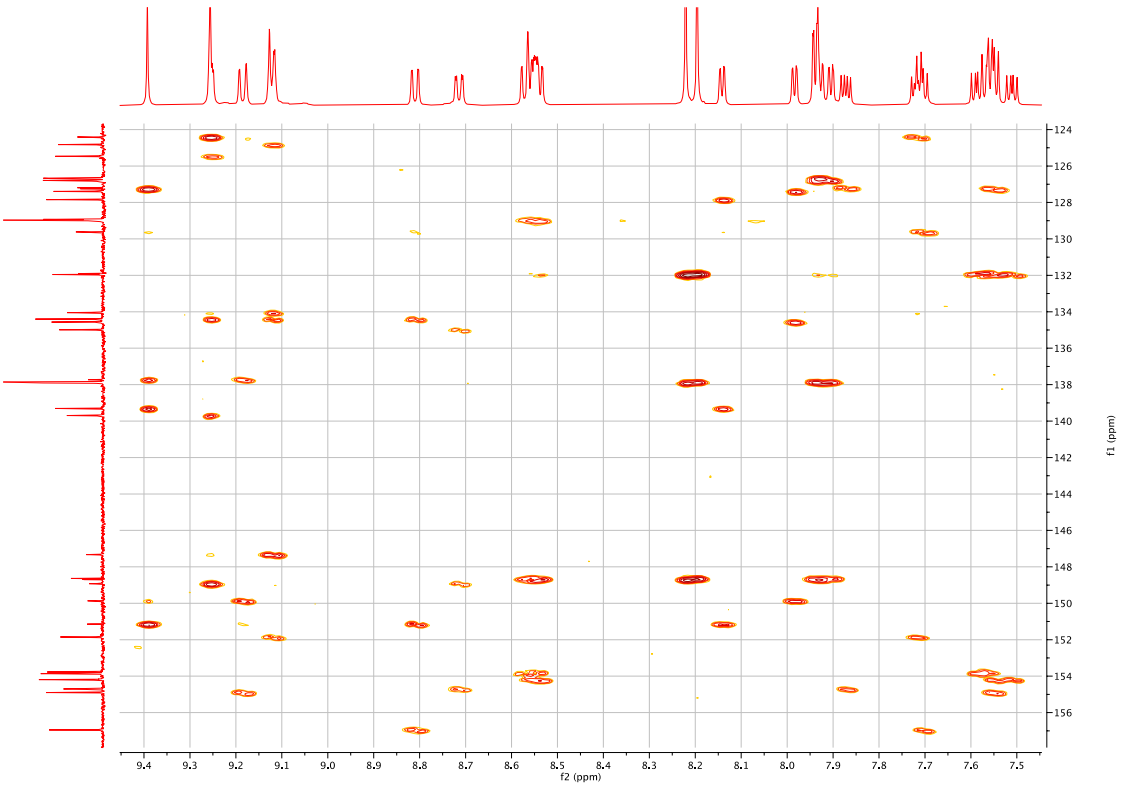

Fig. S29 HMBC NMR of **Ru-PSO$_2$P** (CD_3CN, 600 MHz, 25 °C).

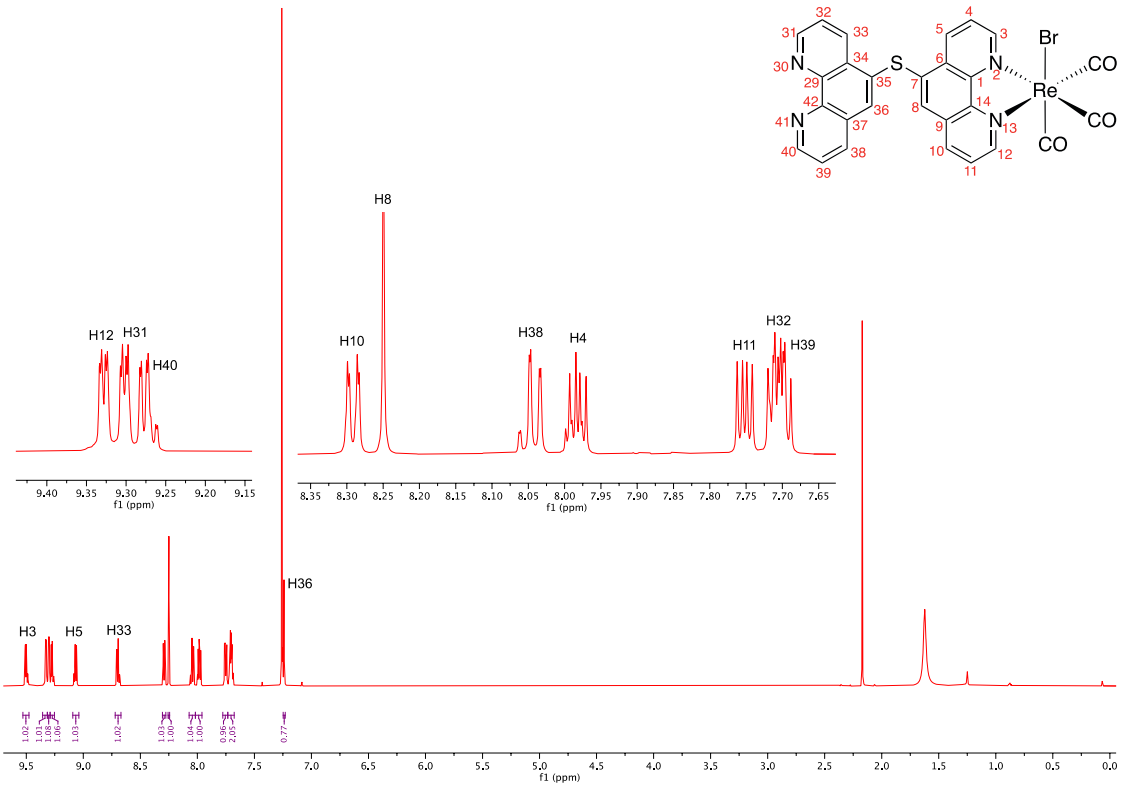

Fig. S30 ^{1}H NMR of **Re-PSP** ($CDCl_3$, 600 MHz, 25 °C).

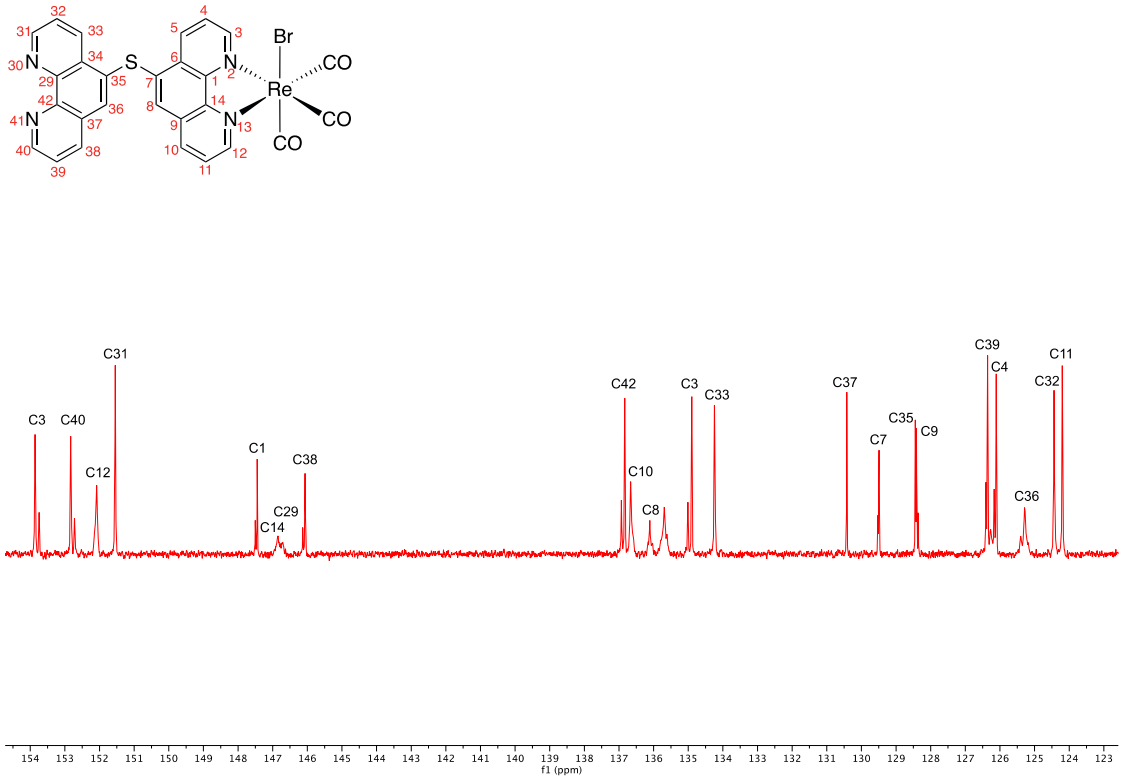

Fig. S31 $^{13}C\{^{1}H\}$ NMR of **Re-PSP** ($CDCl_3$, 151 MHz, 25 °C).

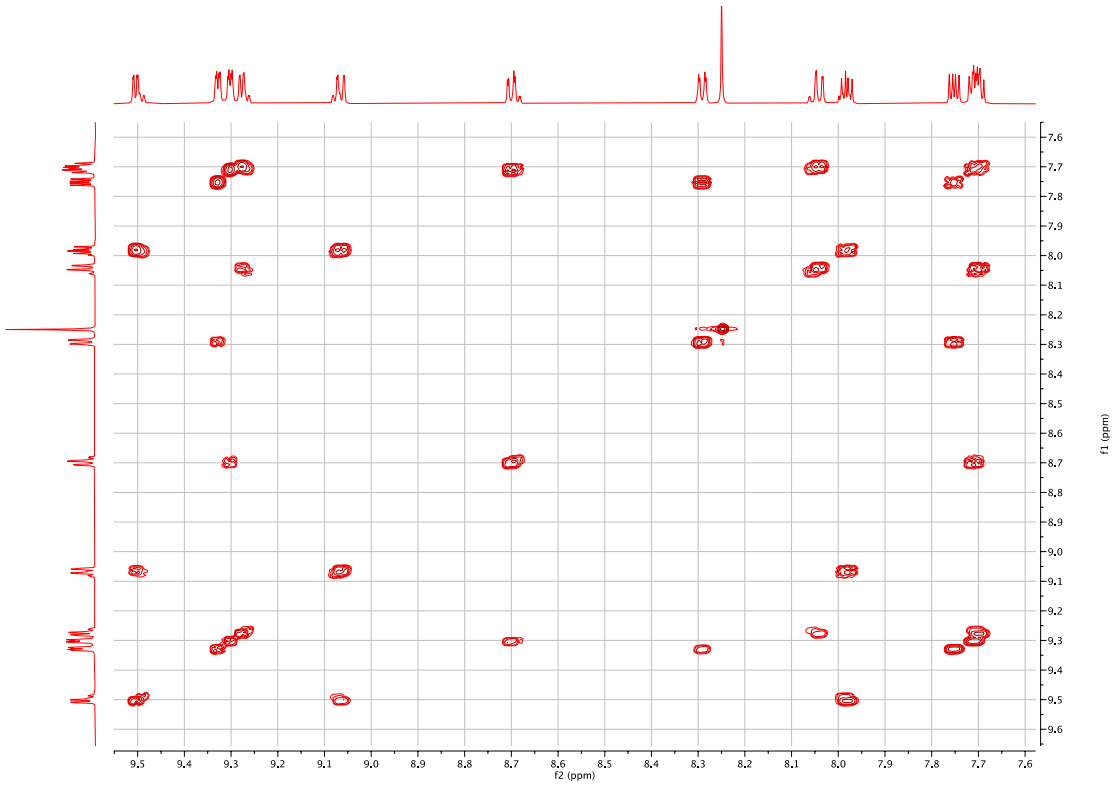

Fig. S32 COSY NMR of **Re-PSP** ($CDCl_3$, 600 MHz, 25 °C).

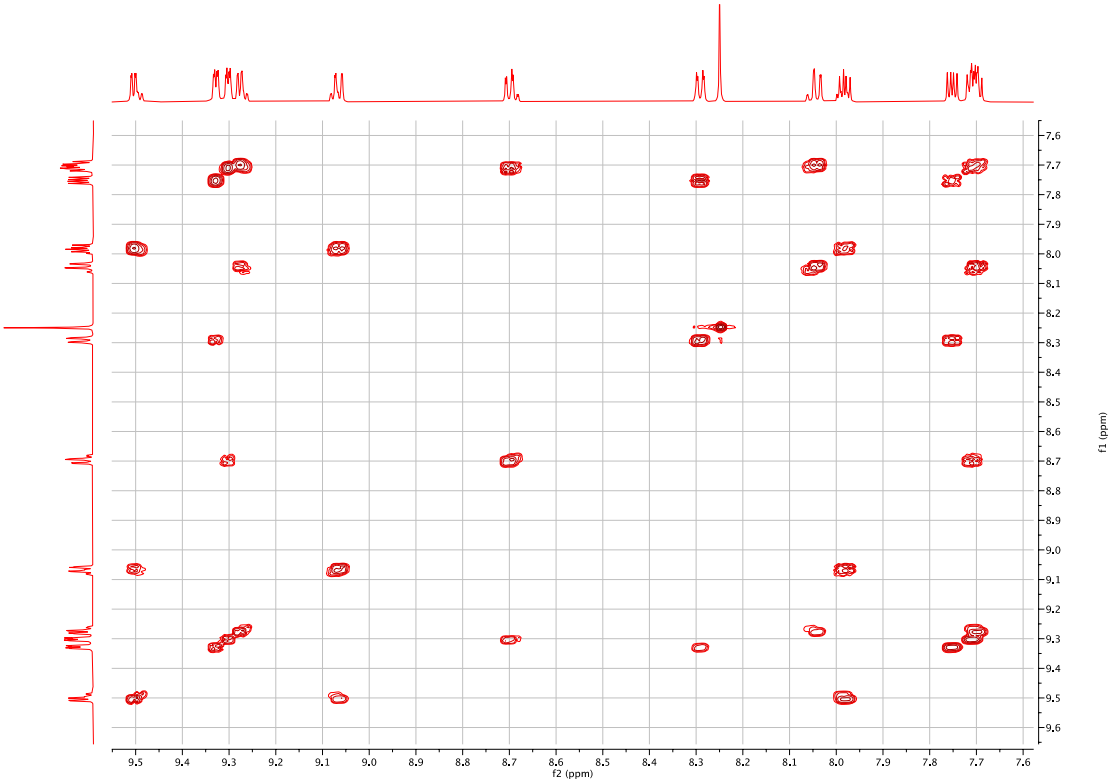

Fig. S33 HSQC NMR of **Re-PSP** ($CDCl_3$, 600 MHz, 25 °C).

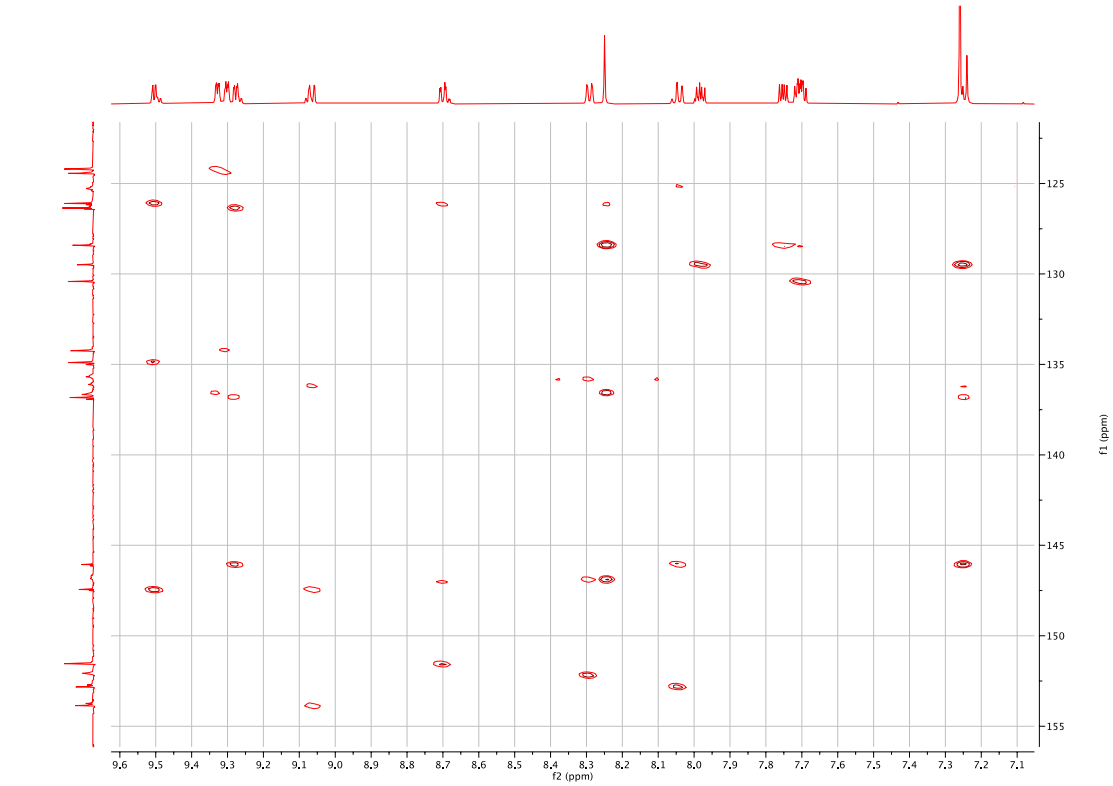

Fig. S34 HMBC NMR of **Re-PSP** ($CDCl_3$, 600 MHz, 25 °C).

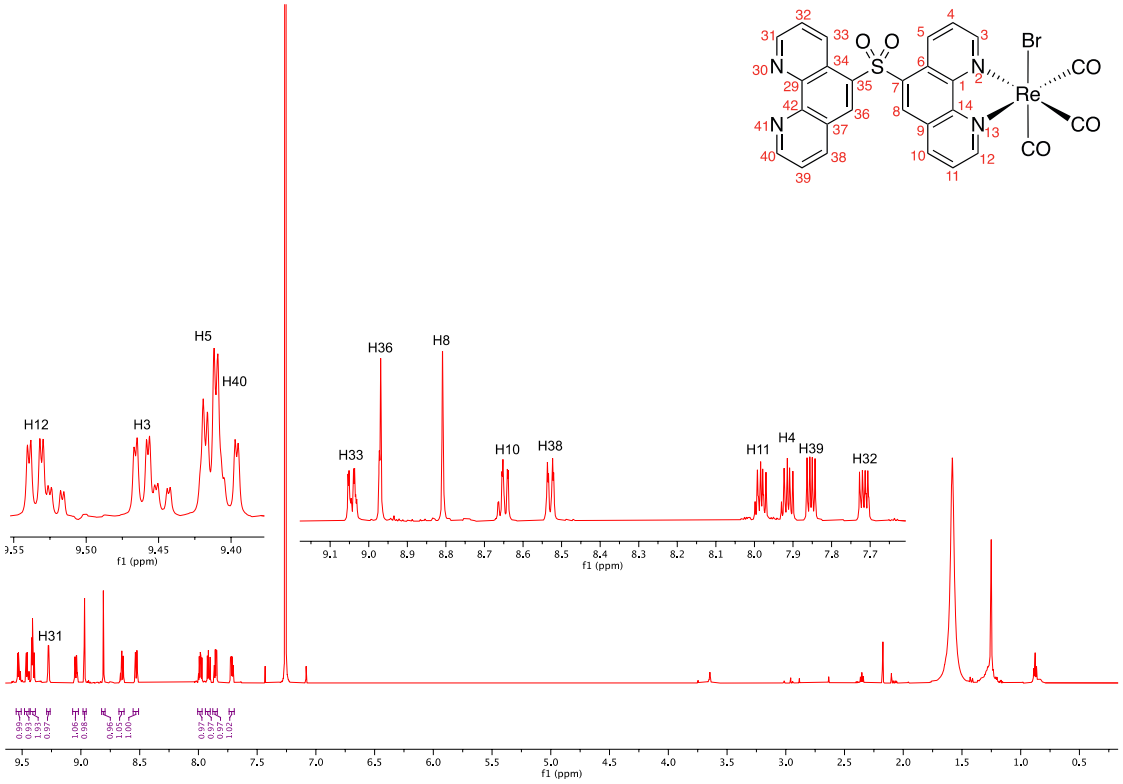

Fig. S35 ^{1}H NMR of **Re-PSO$_2$P** ($CDCl_3$, 600 MHz, 25 °C).

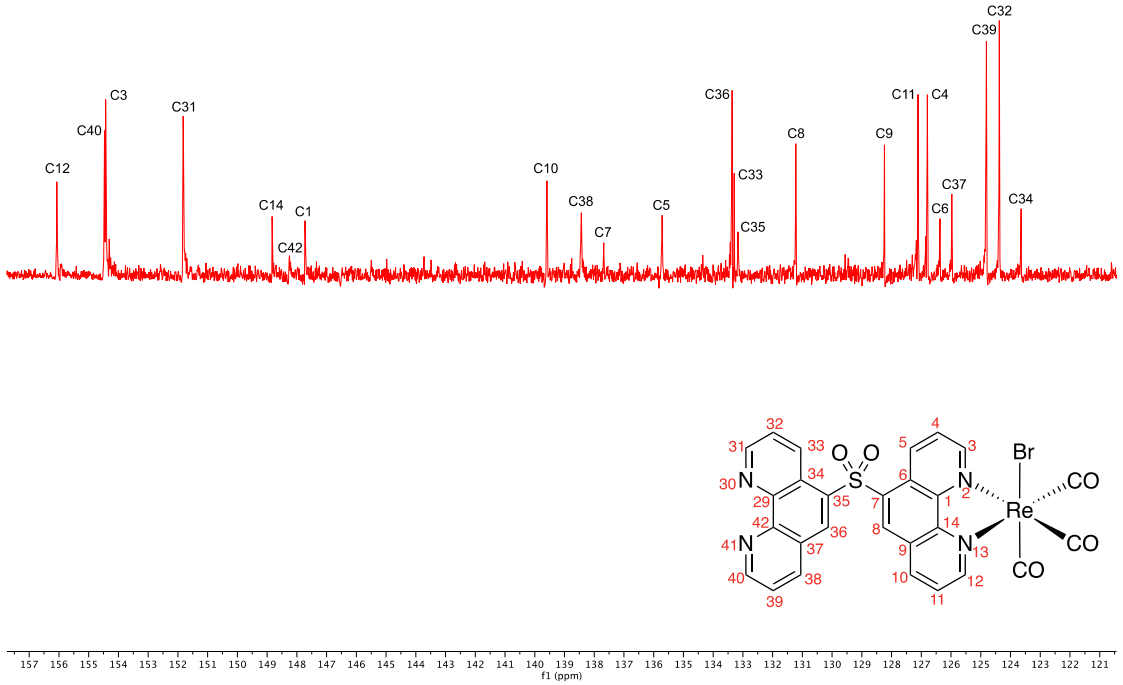

Fig. S36 ^{13}C{^{1}H} NMR of **Re-PSO$_2$P** ($CDCl_3$, 151 MHz, 25 °C).

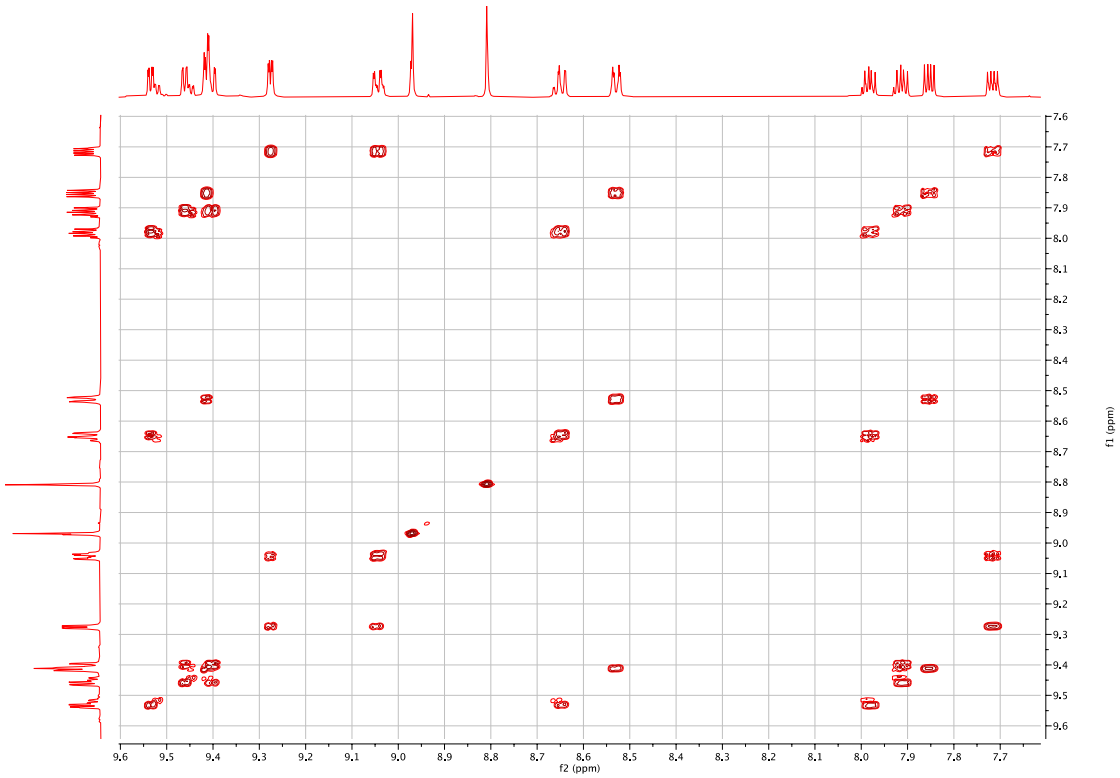

Fig. S37 COSY NMR of **Re-PSO$_2$P** ($CDCl_3$, 600 MHz, 25 °C).

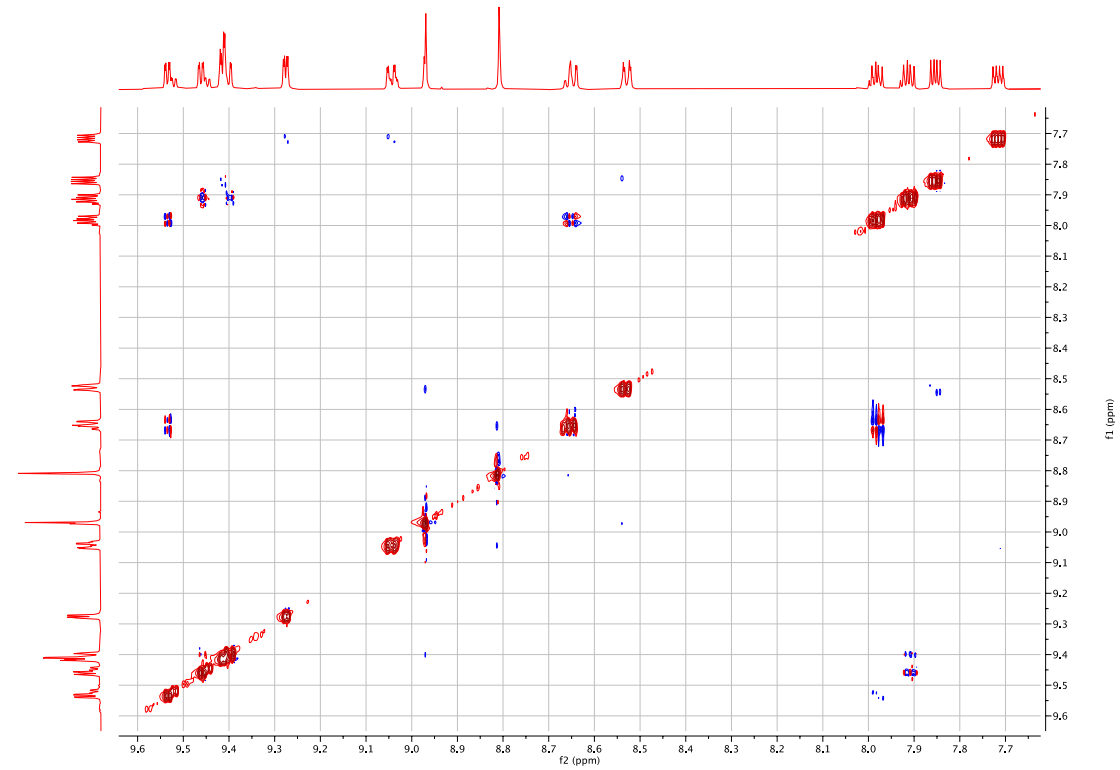

Fig. S38 ROESY NMR of **Re-PSO$_2$P** ($CDCl_3$, 600 MHz, 25 °C).

Fig. S39 HSQC NMR of **Re-PSO$_2$P** ($CDCl_3$, 600 MHz, 25 °C).

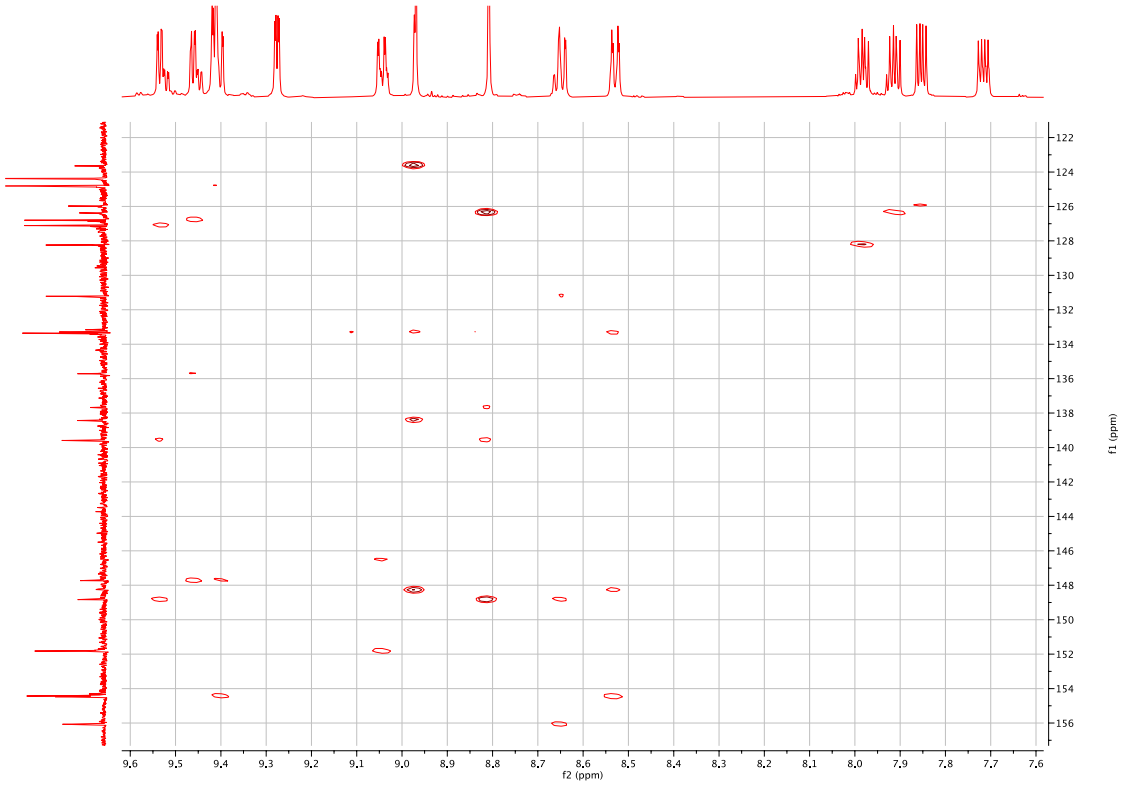

Fig. S40 HMBC NMR of **Re-PSO$_2$P** ($CDCl_3$, 600 MHz, 25 °C).

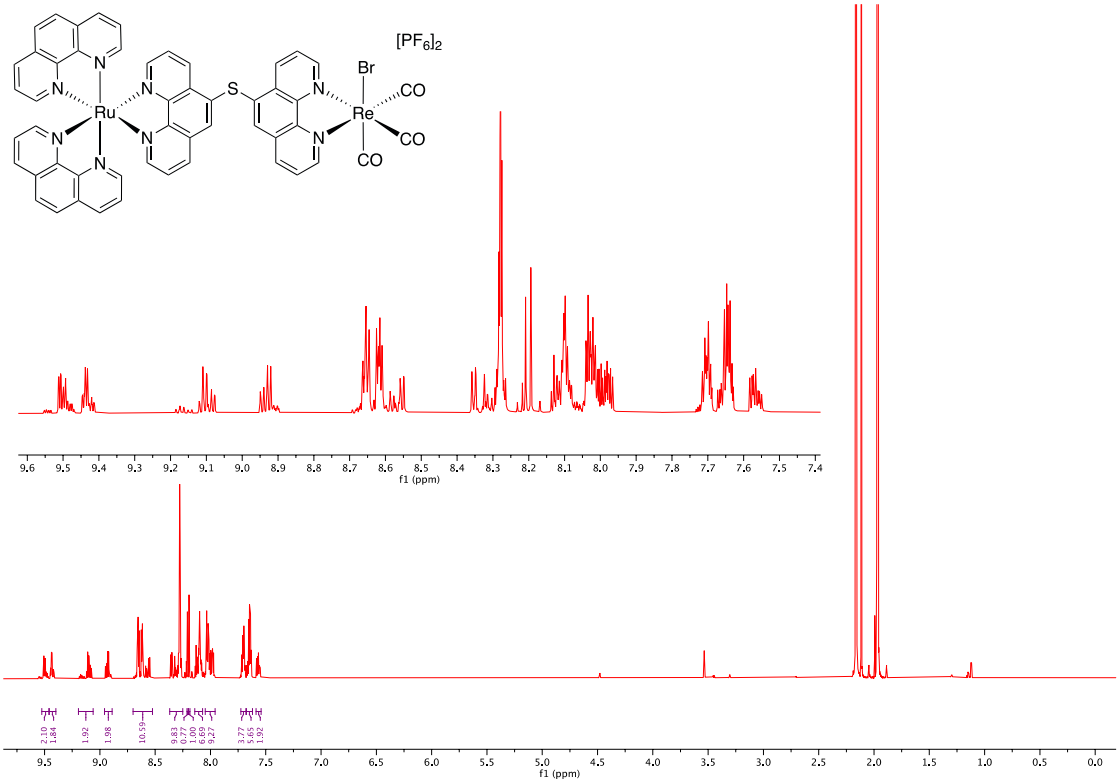

Fig. S41 ^{1}H NMR of **Ru-PSP-Re** (CD_3CN, 850 MHz, 25 °C).

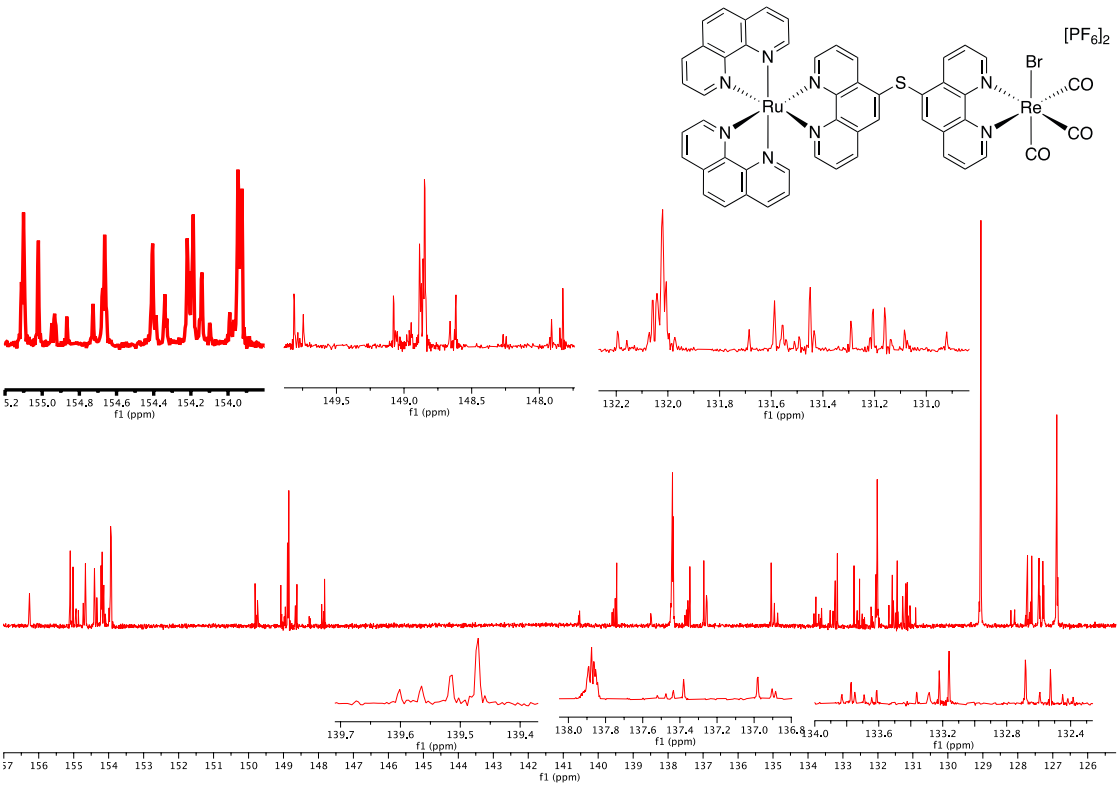

Fig. S42 $^{13}C\{^{1}H\}$ NMR of **Ru-PSP-Re** (CD_3CN, 214 MHz, 25 °C).

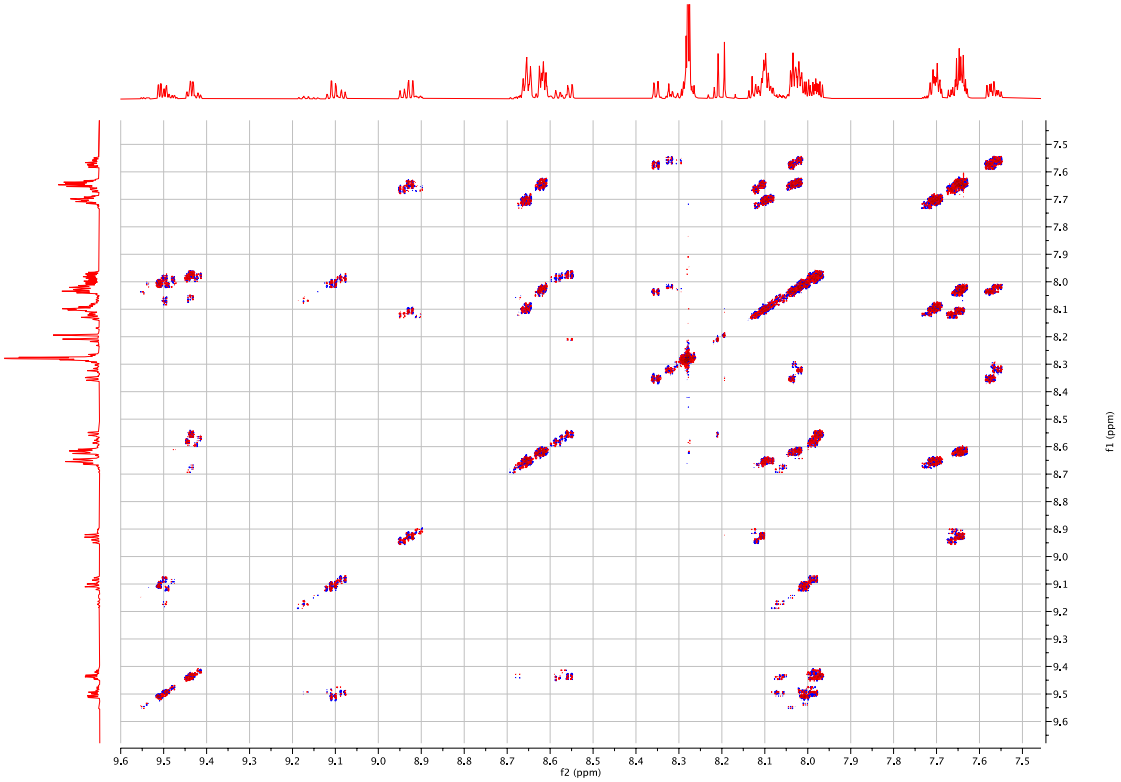

Fig. S43 COSY NMR of **Ru-PSP-Re** (CD_3CN, 850 MHz, 25 °C).

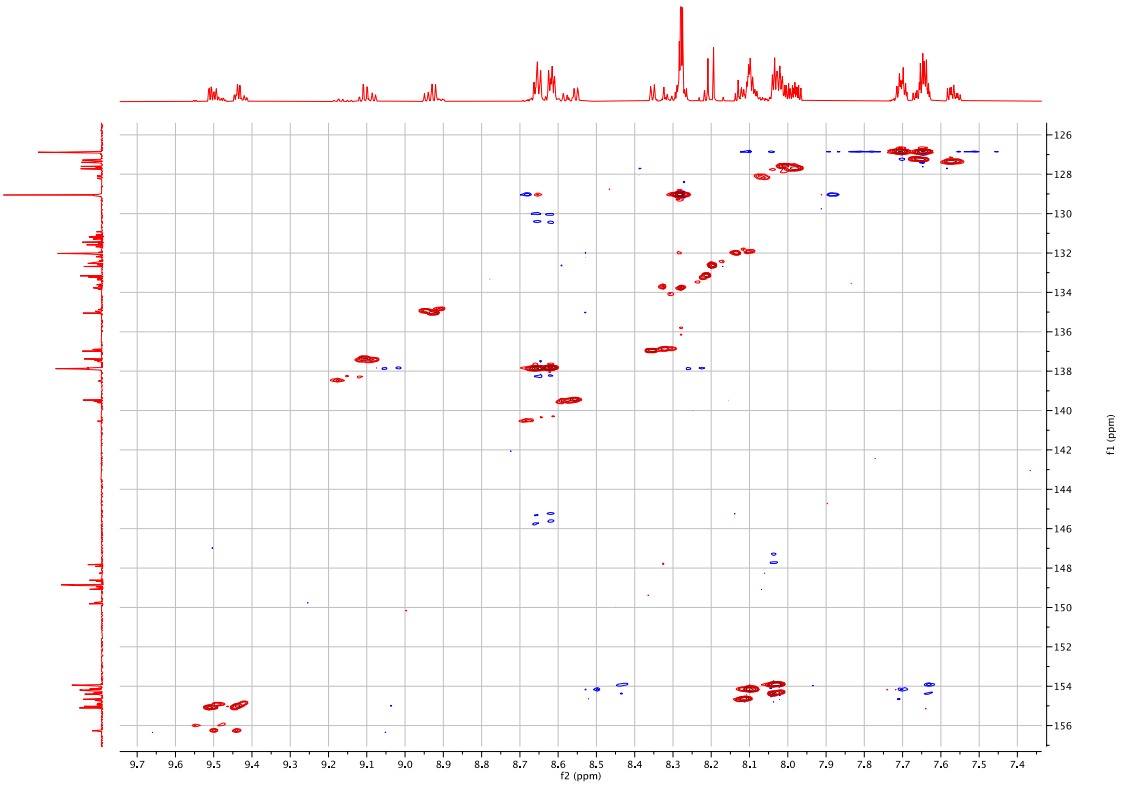

Fig. S44 HSQC NMR of **Ru-PSP-Re** (CD_3CN, 850 MHz, 25 °C).

Fig. S45 HMBC NMR of **Ru-PSP-Re** (CD_3CN, 850 MHz, 25 °C).

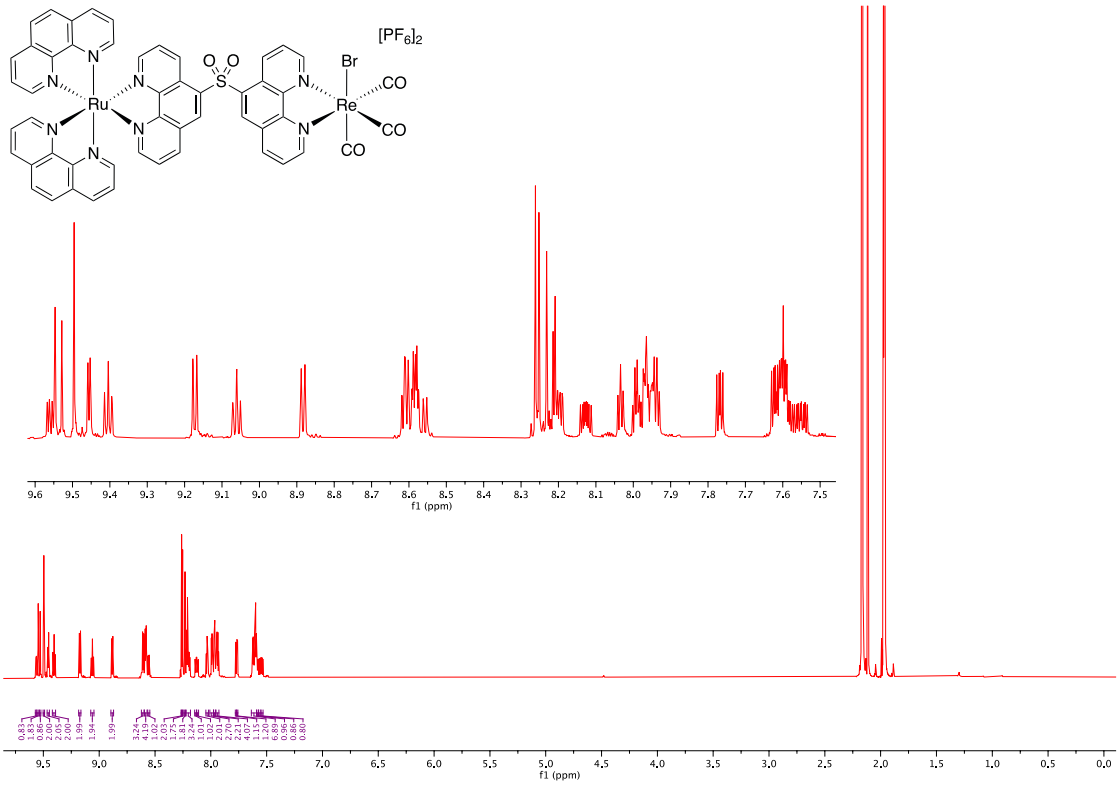

Fig. S46 ^1H NMR of **Ru-PSO$_2$P-Re** (CD_3CN, 850 MHz, 25 °C).

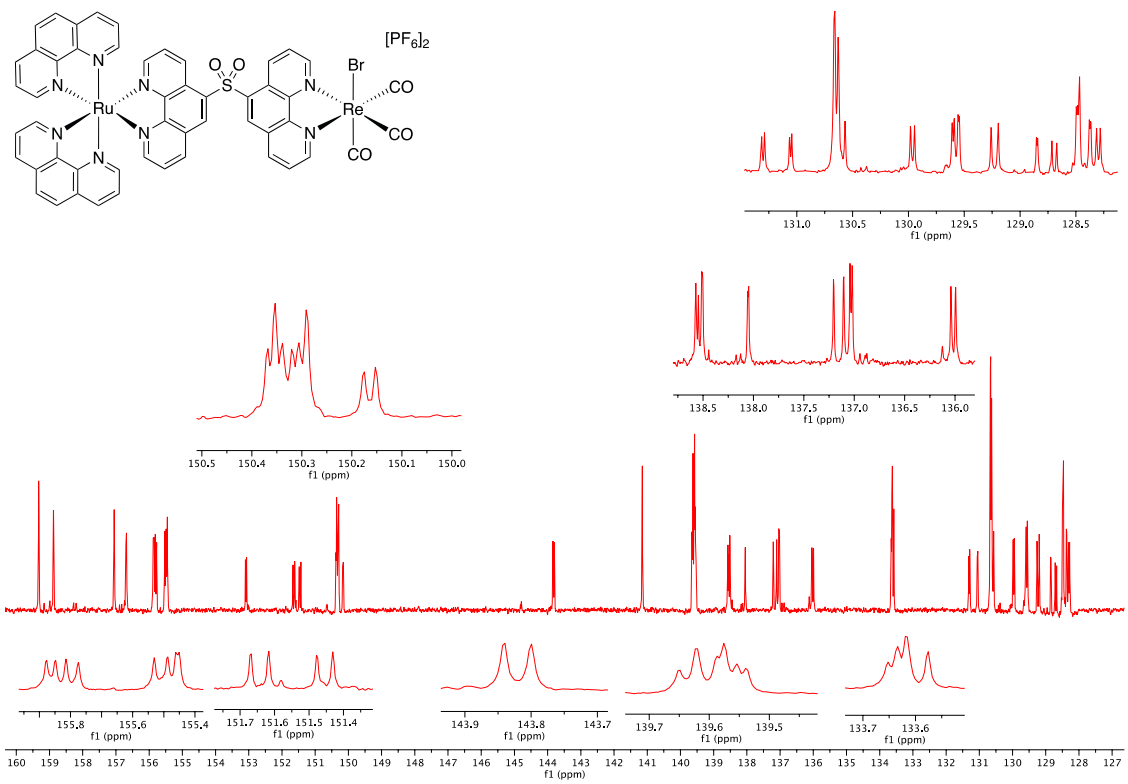

Fig. S47 $^{13}C\{^{1}H\}$ NMR of **Ru-PSO$_2$P-Re** (CD_3CN, 214 MHz, 25 °C).

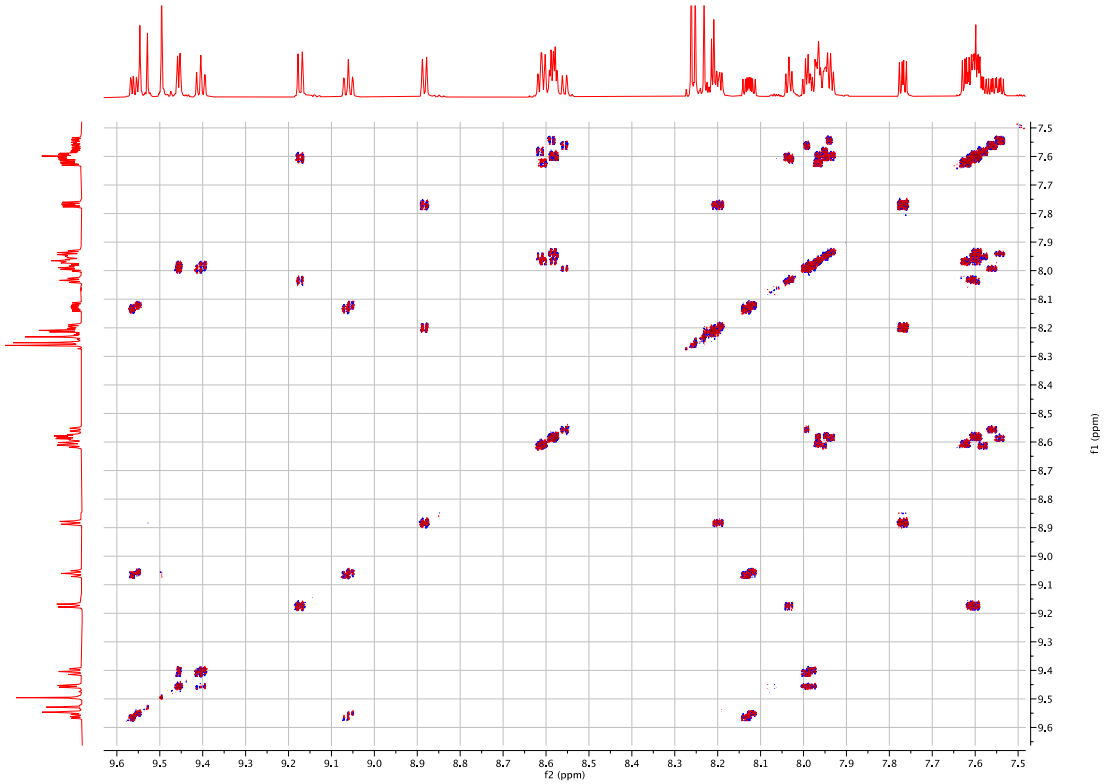

Fig. S48 COSY NMR of **Ru-PSO$_2$P-Re** (CD_3CN, 850 MHz, 25 °C).

Fig. S49 ROESY NMR of **Ru-PSO$_2$P-Re** (CD_3CN, 850 MHz, 25 °C).

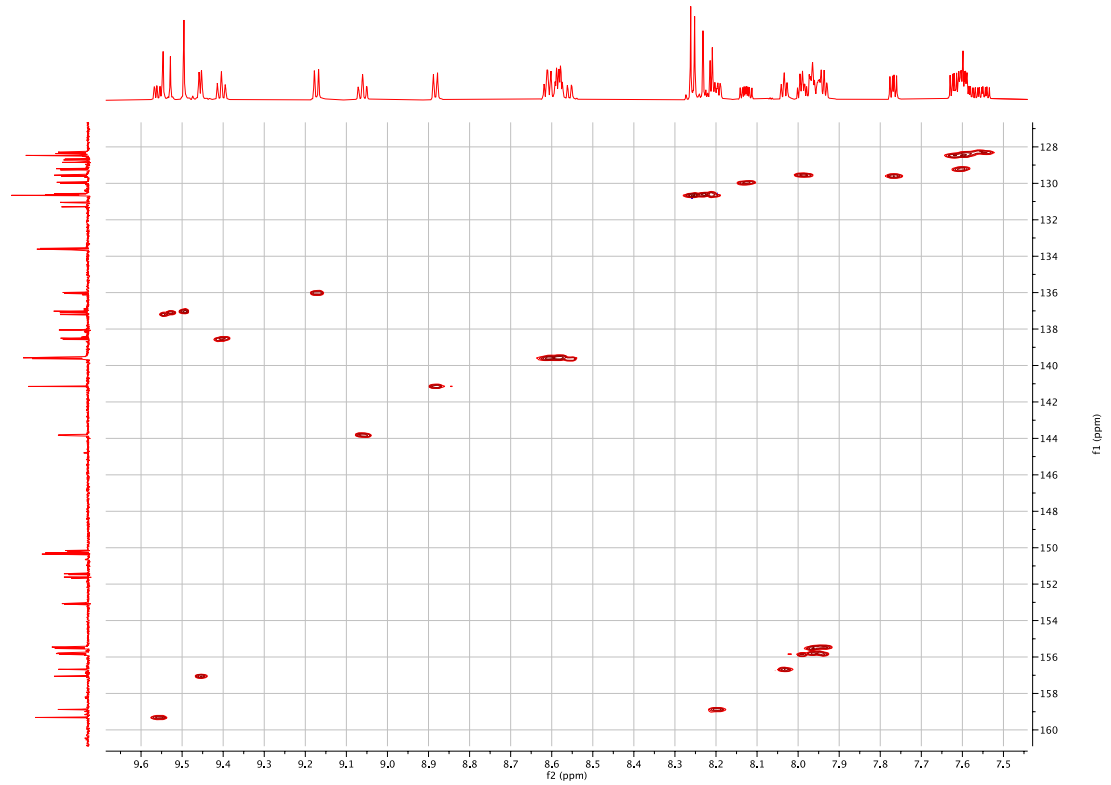

Fig. S50 HSQC NMR of **Ru-PSO$_2$P-Re** (CD_3CN, 850 MHz, 25 °C).

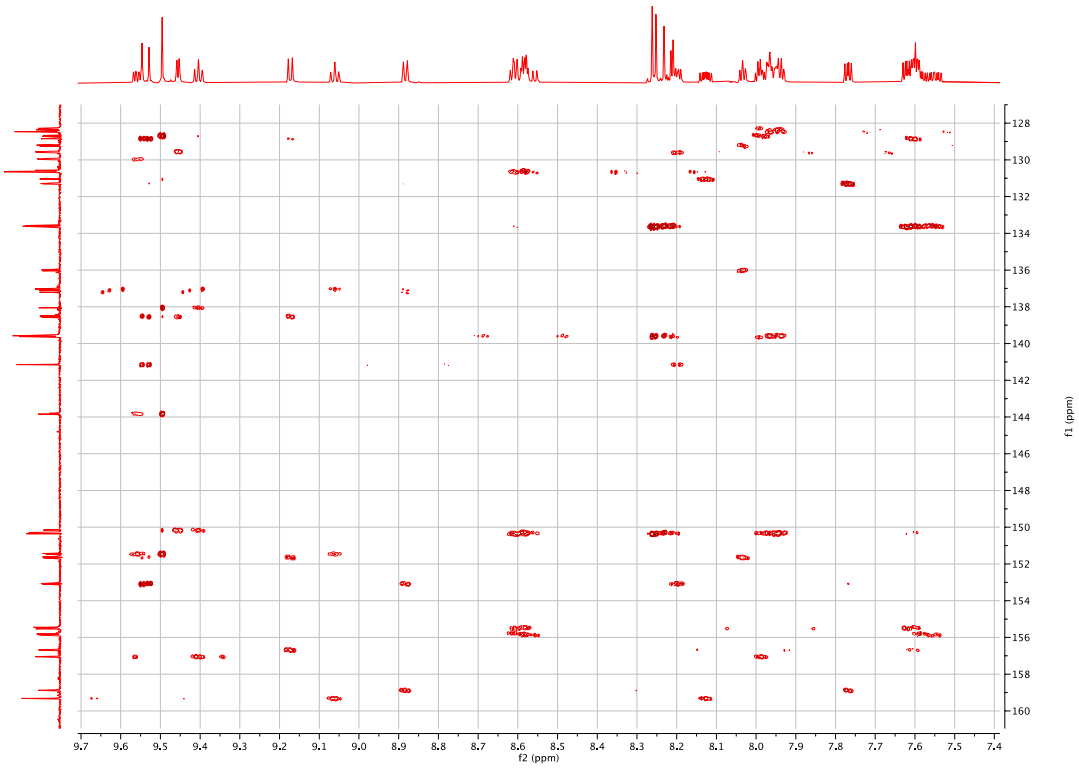

Fig. S51 HMBC NMR of **Ru-PSO$_2$P-Re** (CD_3CN, 850 MHz, 25 °C).

References

1 B. P. Sullivan, D. J. Salmon and T. J. Meyer, *Inorg. Chem.*, 1978, **17**, 3334–3341.

2 I. S. H. Lee, E. H. Jeoung and M. M. Kreevoy, *J. Am. Chem. Soc.*, 1997, **119**, 2722–2728.

3 P. Kurz, B. Probst, B. Spingler and R. Alberto, *Eur. J. Inorg. Chem.*, 2006, 2966–2974.

4 D. J. Frisch, M. J.; Trucks, G. W.; Schlegel, H. B.; Scuseria, G. E.; Robb, M. A.; Cheeseman, J. R.; Scalmani, G.; Barone, V.; Petersson, G. A.; Nakatsuji, H.; Li, X.; Caricato, M.; Marenich, A. V.; Bloino, J.; Janesko, B. G.; Gomperts, R.; Mennucci, B.; Hratch, 2016.

5 C. Adamo and V. Barone, *J. Chem. Phys.*, 1999, **110**, 6158–6170.

6 T. H. Dunning Jr. and P. J. Hay, in *Modern Theoretical Chemistry*, ed. H. F. Schaefer II, Plenum, New York, 3rd edn., 1977, pp. 1–28.

7 P. J. Hay and W. R. Wadt, *J. Chem. Phys.*, 1985, **82**, 270–283.

8 P. J. Hay and W. R. Wadt, *J. Chem. Phys.*, 1985, **82**, 299–310.

9 W. R. Wadt and P. J. Hay, *J. Chem. Phys.*, 1985, **82**, 284–298.

10 S. Leonid, Chemissian V 4.53, http://www.chemissian.com.

11 M. Cossi, N. Rega, G. Scalmani and V. Barone, *J. Comput. Chem.*, 2003, **24**, 669–681.

12 I. A. Dotsenko, M. Curtis, N. M. Samoshina and V. V. Samoshin, *Tetrahedron*, 2011, **67**, 7470–7478.

13 M. Kirihara, A. Itou, T. Noguchi and J. Yamamoto, *Synlett*, 2010, 1557–1561.

14 M. Jäger, R. J. Kumar, H. Görls, J. Bergquist and O. Johansson, *Inorg. Chem.*, 2009, **48**, 3228–3238.

15 Y. Kuramochi, O. Ishitani and H. Ishida, *Coord. Chem. Rev.*, 2018, **373**, 333–356.